

Triazole-Based Inhibitors of the Wnt/ β -Catenin Signaling Pathway Improve Glucose and Lipid Metabolism in Diet-Induced Obese Mice

Obinna N. Obianom, Yong Ai, yingjun li, Wei Yang, Dong Guo, Hong Yang, Srilatha Sakamuru, Menghang Xia, Fengtian Xue, and Yan Shu

J. Med. Chem., **Just Accepted Manuscript** • DOI: 10.1021/acs.jmedchem.8b01408 • Publication Date (Web): 03 Jan 2019

Downloaded from <http://pubs.acs.org> on January 7, 2019

Just Accepted

“Just Accepted” manuscripts have been peer-reviewed and accepted for publication. They are posted online prior to technical editing, formatting for publication and author proofing. The American Chemical Society provides “Just Accepted” as a service to the research community to expedite the dissemination of scientific material as soon as possible after acceptance. “Just Accepted” manuscripts appear in full in PDF format accompanied by an HTML abstract. “Just Accepted” manuscripts have been fully peer reviewed, but should not be considered the official version of record. They are citable by the Digital Object Identifier (DOI®). “Just Accepted” is an optional service offered to authors. Therefore, the “Just Accepted” Web site may not include all articles that will be published in the journal. After a manuscript is technically edited and formatted, it will be removed from the “Just Accepted” Web site and published as an ASAP article. Note that technical editing may introduce minor changes to the manuscript text and/or graphics which could affect content, and all legal disclaimers and ethical guidelines that apply to the journal pertain. ACS cannot be held responsible for errors or consequences arising from the use of information contained in these “Just Accepted” manuscripts.

1
2
3 **Triazole-Based Inhibitors of the Wnt/ β -Catenin Signaling Pathway Improve**
4
5 **Glucose and Lipid Metabolism in Diet-Induced Obese Mice**
6
7
8
9

10 Obinna N. Obianom,^{#,1} Yong Ai,^{#,1} Yingjun Li,¹ Wei Yang,^{‡,1} Dong Guo,¹ Hong Yang,¹
11
12 Srilatha Sakamuru,² Menghang Xia,² Fengtian Xue^{*,1} and Yan Shu^{*,1,3}
13
14
15
16

17 ¹Department of Pharmaceutical Sciences, University of Maryland School of Pharmacy,
18
19 Baltimore, Maryland 21201, USA
20

21 ²National Center for Advancing Translational Sciences, National Institutes of Health,
22
23 Bethesda, MD 20892-3375, USA
24

25
26 ³School and Hospital of Stomatology, Guangzhou Medical University, Guangzhou
27
28 510140, China
29

30
31 [#]These authors contributed equally to this work.
32

33 [‡]Current address: School of Pharmaceutical Engineering, Jiangsu Food & Pharmaceutical
34
35 Science College, Huaian, Jiangsu, 223005, China
36

37
38 **Correspondence to:*
39

40 *Dr. Fengtian Xue at the Department of Pharmaceutical Sciences, University of Maryland*
41
42 *School of Pharmacy, 20 Penn Street, Baltimore, Maryland 21201, USA; Phone: 410-706-*
43
44 *8521; Email: fxue@rx.umaryland.edu*
45

46
47 *Dr. Yan Shu at the Department of Pharmaceutical Sciences, University of Maryland*
48
49 *School of Pharmacy, 20 Penn Street, Baltimore, Maryland 21201, USA; Phone: 410-706-*
50
51 *7358; Email: yshu@rx.umaryland.edu*
52
53
54
55
56
57

ABSTRACT

Wnt/ β -catenin signaling pathway is implicated in the etiology and progression of metabolic disorders. While lines of genetic evidence suggest that blockage of this pathway yields favorable outcomes in treating such ailments, few inhibitors have been used to validate the promising genetic findings. Here, we synthesized and characterized a novel class of triazole-based Wnt/ β -catenin signaling inhibitors, and assessed their effects on energy metabolism. One of the top inhibitors, compound **3a**, promoted Axin stabilization, which led to the proteasome degradation of β -catenin and subsequent inhibition of the Wnt/ β -catenin signaling in cells. Treatment of hepatocytes and high fat diet-fed mice with compound **3a** resulted in significantly decreased hepatic lipid accumulation. Moreover, compound **3a** improved glucose tolerance of high fat diet-fed mice without noticeable toxicity, while downregulating the genes involved in the glucose and fatty acid anabolism. The new inhibitors are expected to be further developed for the treatment of metabolic disorders.

INTRODUCTION

The Wnt/ β -catenin pathway plays a pivotal role in cell proliferation, differentiation and growth.¹ It regulates the expression of target genes through the transcriptional factor β -catenin that forms a cytoplasmic “destruction complex” with other proteins including Axin and adenomatous polyposis coli (APC). This complex facilitates the phosphorylation of β -catenin by casein kinase 1 α (CK1 α) and glycogen synthase kinase 3 β (GSK3 β), leading to proteasome degradation of β -catenin during the “off state” of the pathway. The “on-state”, on the other hand, involves enhanced stability and accumulation of β -catenin in the cytoplasm, resulting in its increased translocation to the nucleus where it binds to LEF/TCF transcriptional factors and activates the expression of target genes. Wnt/ β -catenin pathway crosstalks with many other pathways *via* key proteins such as β -catenin, Axin, and GSK3 β .^{1,2} Given the crucial function of Wnt/ β -catenin pathway, it is not surprising that a strong link between this pathway and metabolic disorders has been recognized in recent years.³⁻⁵

The association of the Wnt/ β -catenin pathway to metabolic disorders was first established by the identification of a human polymorphism (*rs7903146*) in the *TCF7L2* gene, which encodes a major nuclear partner protein of β -catenin, as a strong risk factor for type-2 diabetes.⁶ This polymorphism has been known to enhance *TCF7L2* transcription.⁷⁻⁹ Later, Savic *et al* showed that partial knockdown of *Tcf7l2* results in metabolic phenotypes of smaller body weights, decreased fasting glucose, and improved glucose tolerance in mice.¹⁰ We have published similar observations in mice with the genetic haploinsufficiency of *Tcf7l2*.¹¹ However, the role of *TCF7L2* in maintaining metabolic homeostasis in specific tissues remains controversial. *TCF7L2* knockdown was

1
2
3 reported to increase glucose production and gluconeogenic gene expression in cultured
4 hepatocytes,¹² and the transgenic mice overexpressing a dominant negative *Tcf712* mutant
5 in the proglucagon gene-expressing cells exhibited defective glucose homeostasis.¹³
6
7 However, Boj *et al* reported that liver-specific *Tcf712* knockout led to reduced hepatic
8 glucose production during fasting and improved glucose homeostasis in adult mice on a
9 high-fat diet.¹⁴ Recently, Thompson *et al* reported that liver-specific knockout of β -catenin
10 led to a striking protection from fibrosis and liver injury in mice,¹⁵ while Popov *et al*
11 showed that the hepatic downregulation of β -catenin by anti-sense oligonucleotides could
12 improve insulin sensitivity and glucose tolerance in mice.¹⁶ Therefore, although the exact
13 role of the Wnt/ β -catenin pathway in metabolism is yet to be illustrated, overall evidence
14 indicates that downregulation of Wnt/ β -catenin signaling may provide a new therapeutic
15 strategy for the treatment of metabolic disorders such as fatty liver diseases and diabetes.
16
17
18
19
20
21
22
23
24
25
26
27
28
29
30

31 Therapeutics targeting the Wnt/ β -catenin signaling pathway is still in a state of
32 infancy. One reason is that this pathway is bewilderingly complex, with crosstalks to
33 numerous others.¹⁷⁻¹⁹ In addition, because of the severe phenotypes observed in genetic
34 knockout animal models,²⁰ safety concern is historically present. Approximately one dozen
35 of Wnt/ β -catenin pathway inhibitors with distinct mechanisms have been discovered.²¹⁻³³
36 For example, porcupine inhibitors (e.g., LGK-974, Figure 1) decrease the secretion of the
37 Wnt ligands.³⁴ At the plasma membrane, the inhibition of LRP5/6 binding to Wnt proteins
38 by inhibitors such as niclosamide and salinomycin can curb the amount of active β -
39 catenin.^{22,35} In the cytoplasm, stabilization of the destruction complex (e.g., tankyrase
40 inhibitor XAV939²⁵ and CK1 α activator pyrvinium³⁶) can also attenuate β -catenin levels.
41
42 Of note, the safety concern about Wnt inhibitors has not been borne out either preclinically
43
44
45
46
47
48
49
50
51
52
53
54
55
56
57
58
59
60

1
2
3 or clinically, and recently the β -catenin/CBP inhibitor PRI-724 has entered clinical trials
4 as a potential new treatment of various cancers.¹⁷ Several FDA-approved drugs, such as
5 glucocorticoids, retinoids, and celecoxib, are also found to be Wnt/ β -catenin pathway
6 inhibitors.^{17,19} Interestingly, Wnt/ β -catenin pathway inhibitors have emerged to replicate
7 the metabolic outcomes of the above-mentioned genetic manipulation in mice. The CK2
8 inhibitor CX-4945 has been shown to cause mice to be resistant to high fat diet-induced
9 obesity and metabolic disorders.^{37,38} Treatment of mice with a selective tankyrase inhibitor
10 G007-LK has resulted in profound improvement of glucose tolerance and insulin
11 sensitivity.³⁹ However, further studies are needed to fully establish the applicability of
12 these small molecule inhibitors in the treatment of metabolic disorders.
13
14
15
16
17
18
19
20
21
22
23
24
25
26

27 Herein we report a series of novel Wnt/ β -catenin pathway inhibitors based upon a
28 triazole scaffold (Figure 1). New compounds were designed by modifying the chemical
29 structure of pyrvinium, an FDA approved anthelmintic effective for pinworm infection.
30 The drug has been reported to inhibit Wnt signaling with a high potency³⁶. However,
31 further development of pyrvinium as a therapeutic agent for metabolic disorders is
32 prohibited by several reasons related to its chemical structure. Pyrvinium possesses a
33 permanently charged *N*-methylquinolone group that causes extremely low bioavailability
34 of the compound.⁴⁰ The double bond connecting the two ring systems leads to poor
35 solubility. Moreover, the 2,5-dimethyl-1-phenyl-1*H*-pyrrole is prone to oxidation⁴¹ and
36 known as one of the pan assay interference compounds (PAINS).⁴² Herein we describe the
37 synthesis of new inhibitors **3a-3u** employing a neutral aromatic amino group, an amide
38 linker, and a substituted triazole core. Several of the new compounds showed excellent
39 inhibitory potency against Wnt signaling. One of the new compounds, **3a**, was further
40
41
42
43
44
45
46
47
48
49
50
51
52
53
54
55
56
57
58
59
60

characterized by various *in vitro* and *in vivo* biological assays. Compound **3a** showed improved bioavailability, promising efficacy against diet-induced metabolic disorders in mice. In addition, compound **3a** was well tolerated in mice without any notable toxicity.

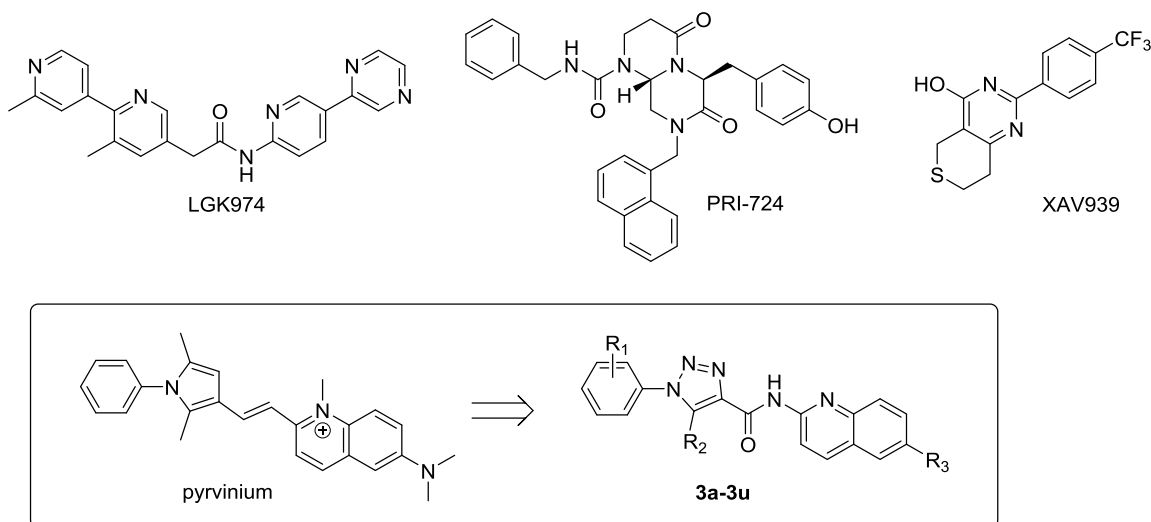
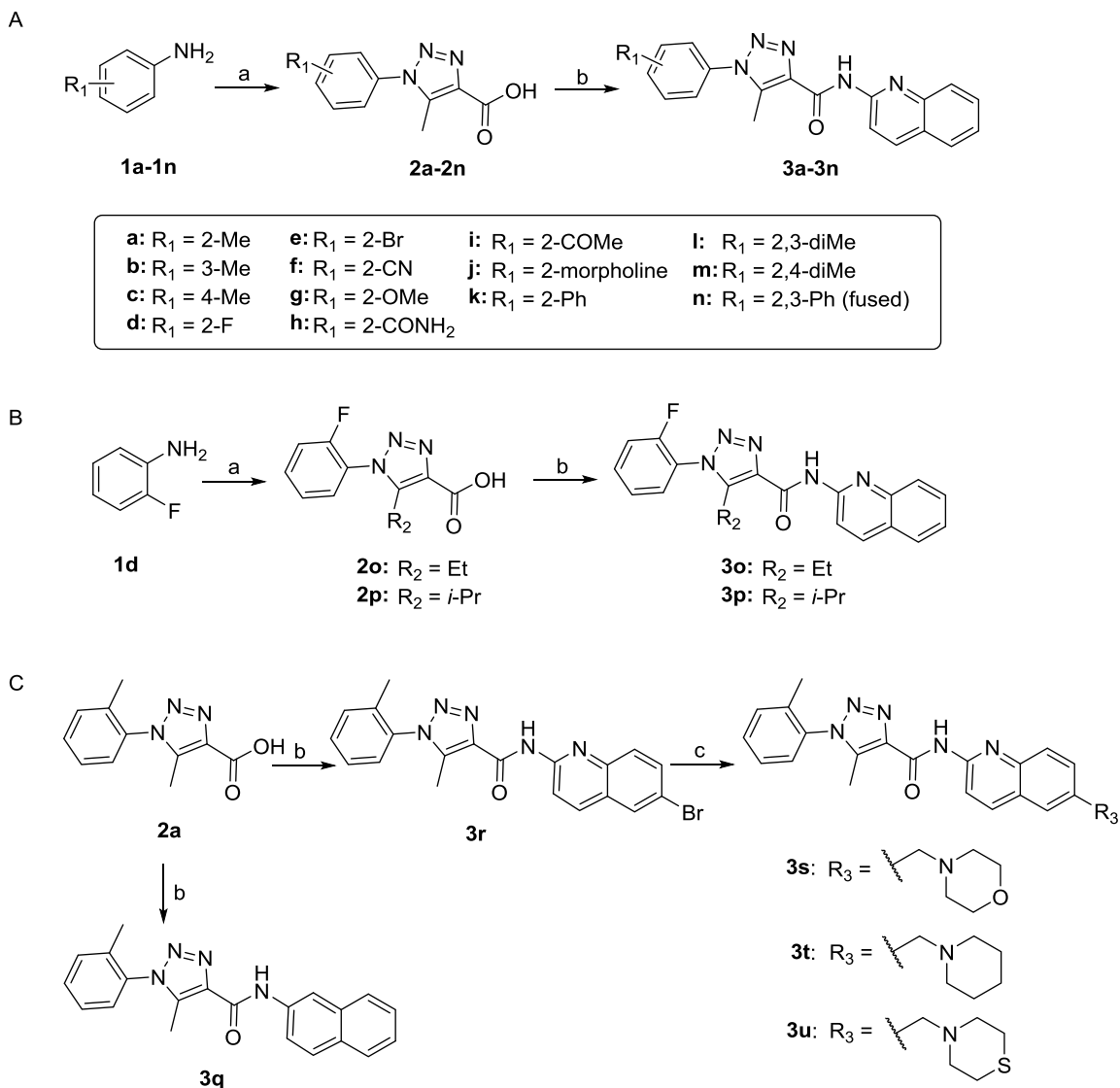


Figure 1. Structures of known Wnt/ β -catenin pathway inhibitors LGK974, PRI724, XAV939, pyrvinium, and the design of new triazole-based inhibitors **3a-3u**.

RESULTS AND DISCUSSION

Synthesis. The synthesis of compounds **3a-3u** is detailed in Scheme 1. Diazotization of the amino group of anilines **1a-1n** using sodium nitrite (NaNO_2) and aqueous HCl, followed by the treatment of the intermediate with sodium azide (NaN_3) gave azides, which underwent cyclization with β -ketoester in EtONa/EtOH yielded triazole-3-carboxylic acids **2a-2p**. Next, PyCIU-mediated coupling of compounds **2a-2p** with various aromatic amines in dichloroethane (DCE) provided target compounds **3a-3r** in moderate to good yields. Finally, Pd-catalyzed cross-coupling of compound **3r** with various potassium trifluoroborate derivatives yielded products **3s-3u** in good yields.

Scheme 1. Synthesis of compounds **3a-3u**^a

^aReagents and conditions: (a) (i) NaNO₂, HCl, NaN₃, H₂O, 0 °C; (ii) ethyl 3-oxobutanoate for **2a-2n**, ethyl 3-oxopentanoate for **2o**, ethyl 4-methyl-3-oxopentanoate for **2p**, EtONa, EtOH, 80 °C; (b) 2-aminoquinoline for **3a-3p**, naphthalen-2-amine for **3q**, 6-bromoquinolin-2-amine for **3r**, PyClU, DIPEA, DCE, 80 °C; (c) potassium trifluoroborate derivatives, Pd(OAc)₂, XPhos, Cs₂CO₃, THF/H₂O, 80 °C, 24-48 h.

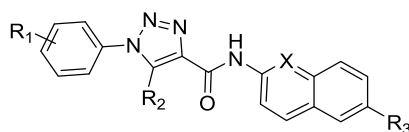
Structure-Activity Relationship. Compound **3a** indicated an excellent IC₅₀ value of 4.1 nM in the luciferase gene reporter assay for Wnt signaling activity, which is over 1,000-fold higher than that of **3b** (3-methyl group) and **3c** (4-methyl group), and 180-fold higher than the parent compound pyrvinium (Table 1). Additional methyl group at the 3- (**3l**) or 4-position (**3m**) of the phenyl ring led to new inhibitors with 34- and 66-fold decreased potencies, respectively. The naphthyl analog **3n** was a weak inhibitor with an IC₅₀ value of 5.5 μM. These results indicated that single *ortho*-substitution is preferred on the phenyl ring. Substitution of the 2-methyl group with various functionalities generated new inhibitors **3d-3k**. Among them, the F-analog (**3d**) demonstrated excellent potency with an IC₅₀ value in the sub-nanomolar range. The Br- (**3e**), NC- (**3f**), and MeO- (**3g**) analogs also showed low nM potencies. However, large substituents such as amide (**3h**), ketone (**3i**), morpholine (**3j**) and Ph (**3k**) turned out to be detrimental to the inhibitory activity.

Next, substitution effects of the triazole core (R₂) were studied using compounds **3o** and **3p**. Compared to inhibitor **3d**, the ethyl analog **3o** was slightly less potent. However with the branched isopropyl group, compound **3p** turned out to be over 20-fold less potent than compound **3d**. These results indicated that small group was preferred at the R₂ position.

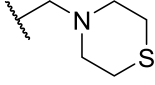
In addition, removal of the quinoline nitrogen yielded compound **3q** that totally lost inhibitory activity. This result highlighted the importance of the quinoline nitrogen in maintaining high potency. Finally, we sought to explore the possibility of expanding the quinoline ring system. The Br-substituted compound **3r** indicated similar potency as that of the parent compound pyrvinium. Similarly, potent inhibitors were obtained when morpholine (**3s**), piperidine (**3t**), or thiomorpholine (**3u**) were included at the same R₃

position. These results indicated that further expansion of the quinoline ring could impair the activity of the inhibitor.

Table 1. Inhibition of Wnt/ β -Catenin Signaling Pathway by Compounds 3a-3u



Cmpds	R ₁	R ₂	R ₃	X	IC ₅₀ (nM) ^a
3a	2-Me	Me	H	N	4.1 ± 0.4
3b	3-Me	Me	H	N	>10,000
3c	4-Me	Me	H	N	>10,000
3d	2-F	Me	H	N	1.2 ± 0.2
3e	2-Br	Me	H	N	7.6 ± 0.3
3f	2-CN	Me	H	N	34 ± 4.3
3g	2-OMe	Me	H	N	18 ± 3.3
3h	2-CONH ₂	Me	H	N	>10,000
3i	2-COMe	Me	H	N	8,800 ± 1322
3j	2-morpholine	Me	H	N	1,900 ± 5.4
3k	2-Ph	Me	H	N	390 ± 68.1
3l	2,3-diMe	Me	H	N	140 ± 5.8
3m	2,4-diMe	Me	H	N	270 ± 23.8
3n	2,3-Ph (fused)	Me	H	N	5,500 ± 1186
3o	2-F	Et	H	N	4.7 ± 0.7
3p	2-F	<i>i</i> -Pr	H	N	25 ± 0.5
3q	2-Me	Me	H	CH	4,900 ± 743
3r	2-Me	Me	Br	N	830 ± 98.2
3s	2-Me	Me		N	1,300 ± 169
3t	2-Me	Me		N	1,200 ± 168

3u	2-Me	Me		N	230 ± 28
pyrvinium					750 ± 137

^aThe values of IC₅₀ for each compound to inhibit the Wnt signaling activity, as determined from the luciferase reporter gene assay, were calculated and data are expressed as mean IC₅₀ (nM) ± SE of each compound from three independent experiments. Note that compounds **3a-3u** did not present any apparent cytotoxicity during the short treatment duration used for the luciferase gene reporter assay (Table S2).

Compound 3a, a Potent Inhibitor of the Wnt/ β -Catenin Signaling Pathway. As model compounds, we next chose compounds **3a** and **3n** and further evaluated them in various biological assays. We chose compound **3a** over the more potent compound **3d** (Table 1) because in the assessment of their potential cytotoxicity in unstimulated normal HEK293 cells with a longer incubation time of 72 h relative to that for the above reporter assay, we found that **3d** was more cytotoxic than **3a** (Figure S1). While compound **3d** was more potent than **3a**, their potencies remained in the same magnitude. Compound **3a** showed superior potency in HEK293 cells in the presence of Wnt signaling activators LiCl and Wnt3a (Figure 2A, B). Compound **3a** inhibited the Wnt/ β -catenin signaling pathway by stabilization of Axin and subsequent β -catenin degradation (Figure 2C-E and Figure S2A-B). Stabilization of Axin was confirmed by the increased cytoplasmic punctas as has been demonstrated previously by other Axin stabilizers.⁴³ The expression of the pathway target genes including *CycD1* and *Axin2* was repressed at the messenger RNA (mRNA) levels. In the presence of LiCl, which activates Wnt/ β -catenin pathway *via* the inhibition of GSK3 β , compound **3a** decreased the cellular level of β -catenin while the inactive analog **3n** had little effect (Figure 2F).

The downregulation of β -catenin levels and the consistent efficacy of compound **3a** in both Wnt3a- and LiCl-conditioned medium suggested a mechanism different from that of the parent compound pyrvinium, whose effect is diminished in the presence of LiCl.³⁶ We performed additional studies with varying concentrations of LiCl, and observed no effect by LiCl in changing the inhibitory potency of compound **3a** towards Wnt/ β -catenin signaling pathway (Figure S2).

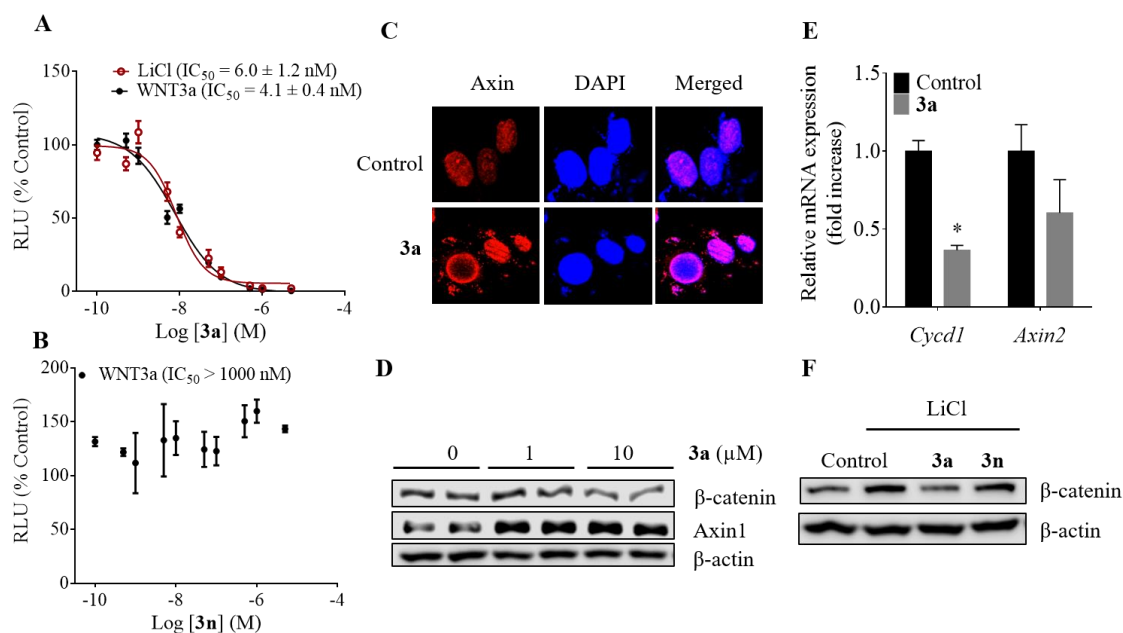


Figure 2. Characterization of compound **3a** as an inhibitor of Wnt/ β -catenin signaling pathway. (A) TCF/LEF responsive luciferase reporter assay in HEK293 cells with varying concentration of compound **3a** and (B) compound **3n** in Wnt3a- or LiCl-conditioned medium. The data were fitted to determine the IC_{50} of inhibition of LiCl- and Wnt3a-induced activation of the Wnt/ β -catenin signaling pathway (mean \pm S.D, $n = 4$). (C) Confocal microscope images of **3a**-treated HEK293 cells for detection of Axin (Axin1). The cells were incubated with 1 μ M of compound **3a** for 14 h. The nucleus was stained by DAPI. (D) Western blot analysis showing the effect of compound **3a** treatment on the

1
2
3 levels of β -catenin and Axin1 proteins in HEK293 cells in the presence of WNT3a. The
4 cells were treated with the compound for 2 h. (E) The mRNA expression of the target
5 genes of Wnt/ β -catenin signaling pathway. The cells were treated for 48 h and harvested
6 with TriZol reagent. * $p < 0.05$. (F) Western blot analysis of HEK293 cells treated with
7 compounds **3a** and **3n** in the presence of lithium chloride for 24 h. RLU- Relative light
8 units.
9

10
11
12 **Mechanism of Wnt/ β -catenin Pathway Inhibition by Compound 3a.** Sequential
13 phosphorylation of β -catenin on residues Ser33, Ser37 and Thr41 by GSK3 β is a critical
14 step in β -catenin degradation. By causing increase in the phosphorylation at these sites,
15 many small molecule Wnt inhibitors facilitate the degradation of β -catenin. To further
16 ascertain if our new inhibitors function through a similar mechanism, we examined the
17 inhibitory potency of compound **3a** in HEK293 cells overexpressed with wild-type and
18 mutant (S33Y) β -catenin (Figure S3). Overexpression of both exogenous β -catenin
19 plasmids led to significant increases in Wnt signaling activities as reflected by the
20 luciferase reporter gene assay, with the S33Y mutant giving a larger increase than the wild
21 type. Nonetheless, compound **3a** inhibited Wnt signaling with a similar potency
22 irrespective of overexpression of either β -catenin, suggesting that the inhibitory effects of
23 compound **3a** may be independent of GSK3 β phosphorylation of at least Ser33 on β -
24 catenin. Note that aside from Ser33 phosphorylation, GSK3 β also phosphorylates Ser37
25 and Thr41 of β -catenin. Thus the mutated β -catenin construct used in our assay may not
26 be sufficient to impair the function of GSK3 β , as immunoprecipitation of β -catenin showed
27 that compound **3a** strengthened the binding of GSK3 β and Axin to β -catenin (Figure 3A).
28
29
30
31
32
33
34
35
36
37
38
39
40
41
42
43
44
45
46
47
48
49
50
51
52
53
54
55
56
57
58
59
60

1
2
3 Thus, the results suggest that compound **3a** treatment may lead to fortification of the
4
5 destruction complex to propagate the degradation of β -catenin.
6
7

8 We next silenced major components of the β -catenin destruction complex, CK1 α ,
9
10 GSK3 β and Axin1, to assess their contribution to the effect of inhibitor **3a**. Only the
11
12 knockdown of CK1 and GSK3 β partially abolished the Wnt inhibitory effect while Axin1
13
14 silencing had no effect on the gene reporter assay of inhibitor **3a** (Figure 3B). Next, we
15
16 performed surface plasmon resonance (SPR) analysis using recombinant CK1 α , GSK3 β ,
17
18 and Axin to determine the binding affinity of compound **3a** to these proteins. We found
19
20 that compound **3a** could not bind to CK1 α and Axin (data not shown), while exhibiting a
21
22 weak binding ($K_D = 4.3 \mu\text{M}$) for recombinant GST-tagged GSK3 β (Figure S4A-C).
23
24 Further, we knocked down GSK3 β and performed the reporter assay for compound **3a**.
25
26 The results show that exclusion of GSK3 β only decreased the effect of compound **3a** by
27
28 1.7 fold (IC_{50} of si-control = 20 nM vs. si-GSK3 β = 34 nM) (Figure S4D). The non-
29
30 correlation of the IC_{50} value from the reporter assay to the K_D of weak binding to GSK3 β
31
32 suggests that GSK3 β is probably not the main target of compound **3a**, although it may play
33
34 a direct role in the inhibitory effect of compound **3a** on Wnt/ β -catenin signaling pathway.
35
36
37
38
39
40

41 In order to determine the inhibitory effect of compound **3a** in other cells bearing
42
43 mutations that lead to an activated Wnt/ β -catenin pathway, we overexpressed the luciferase
44
45 reporter constructs in SW480 and HepG2 cell lines. The SW480 cells have inactivating
46
47 mutations in APC, which lead to ineffective tethering of β -catenin to the destruction
48
49 complex and subsequent increase in cytoplasmic and nuclear β -catenin levels.⁴⁴ In
50
51 contrast, HepG2 cells contain a deletion of the amino acids 25-140 of the *CTNNB1*
52
53 (encoding β -catenin) gene, which includes the binding sites of GSK3 β and CK1 α (Figure
54
55
56
57
58
59
60

3C).⁴⁵ Inhibition of the reporter gene activity by compound **3a** was well observed in SW480 cells, but insignificant in HepG2 cells (Figure 3D). These results suggest the necessity of the full length of β -catenin with intact GSK3 β and CK1 α sites for the inhibitory activity of compound **3a**.

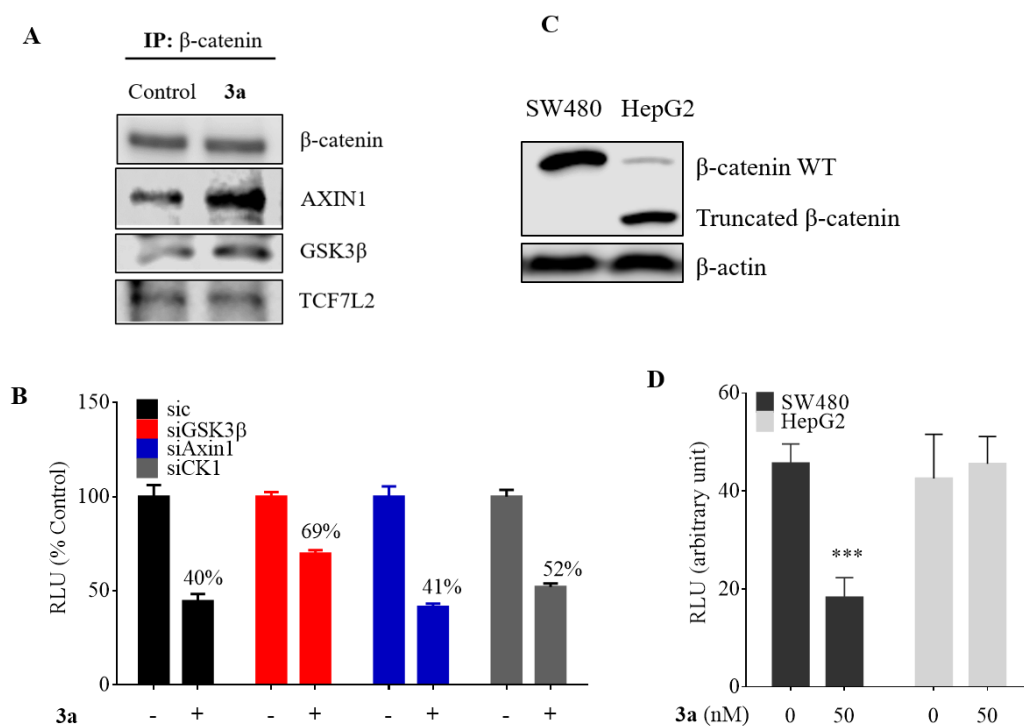


Figure 3. Role of Wnt/ β -catenin pathway effector proteins in the inhibition by compound **3a**. (A) Immunoprecipitation of β -catenin in HEK293 to determine the effect of compound **3a** treatment (12 h) on the interaction of β -catenin with other pathway effector proteins. (B) TCF/LEF gene reporter assay of compound **3a** in the presence of knockdown of GSK3 β , Axin and CK1 α . The HEK293 cells were treated with or without compound **3a** (20 nM) for 24 h. (C) Western blot analysis of protein expression of β -catenin in SW480 and HepG2 cells. (D) TCF/LEF gene reporter assay of SW480 and HepG2 cells treated

1
2
3 with compound **3a**. Data are represented as mean \pm S.D, n = 3. RLU- relative light units.
4
5 *** $p < 0.001$.
6
7

8 **Compound 3a Decreased Lipid Accumulation and Altered the Expression of**
9 **Lipogenic and Gluconeogenic Genes in Hepatocytes.** It has been reported that the
10 Wnt/ β -catenin pathway may play a role in cellular metabolism. Specifically, Axin has been
11 implicated in lipid metabolism. In mice, knockdown of Axin results in significantly
12 increased hepatic lipid accumulation.⁴⁶ Because compound **3a** stabilized the cellular level
13 of Axin, we performed a Nile red staining assay to examine the effect of compound **3a** on
14 lipid accumulation in human hepatic Huh7 cells (Figure 4A). Treatment of the cells with
15 compound **3a** dramatically decreased lipid accumulation. Similar effects were observed
16 by a known Axin stabilizer XAV939. Next, we performed a quantitative PCR to determine
17 the effect of compound **3a** on the gene expression of lipogenesis and gluconeogenesis in
18 mouse hepatocytes. Our results showed that compound **3a** downregulated the mRNA
19 levels of the gluconeogenic (*PEPCK* and *G6PASE*) and lipogenic genes (*FASN*, *ACAA1A*,
20 *ACOT4*, and *SCD1*) (Figure 4B). These results suggested that compound **3a** might
21 decrease the accumulation of lipids in hepatocytes by downregulating gluconeogenic and
22 lipogenic pathways as a consequence of Axin stabilization.
23
24
25
26
27
28
29
30
31
32
33
34
35
36
37
38
39
40
41
42
43
44
45
46
47
48
49
50
51
52
53
54
55
56
57
58
59
60

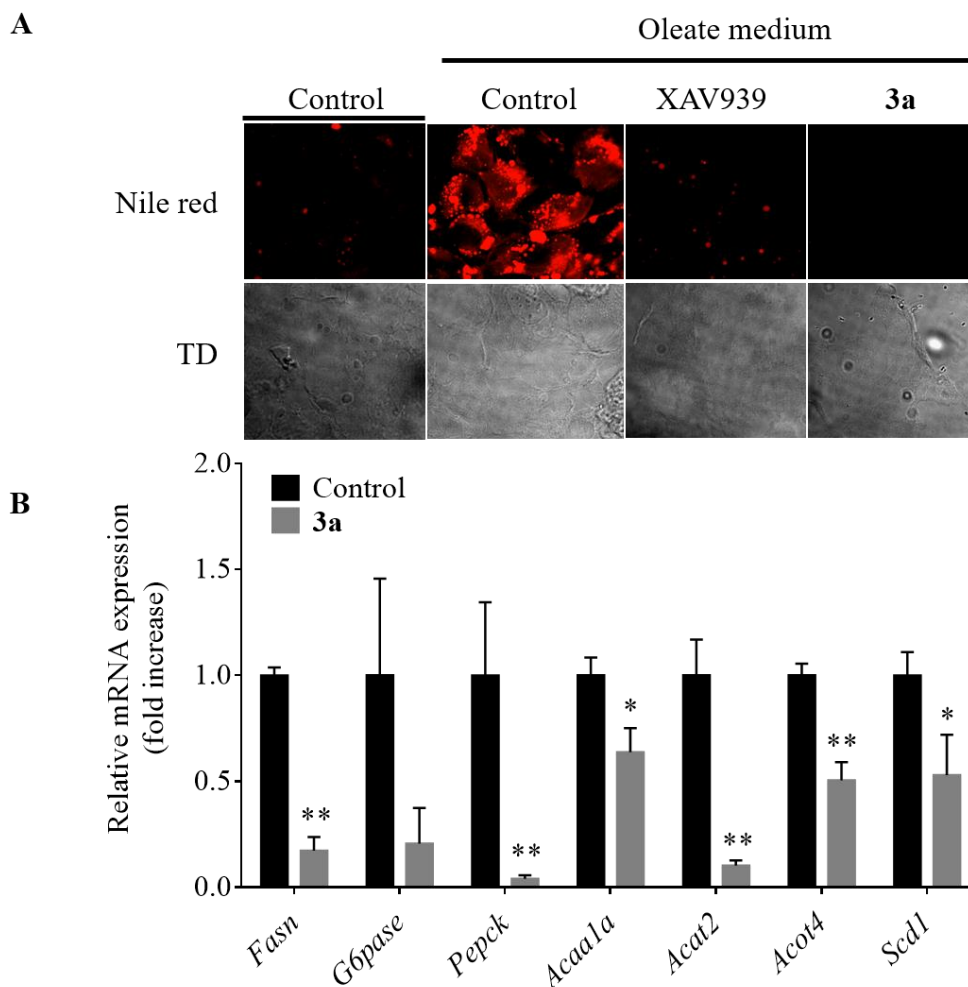


Figure 4. Compound **3a** decreased lipid accumulation and the expression of lipogenic and gluconeogenic genes in hepatocytes. (A) Nile red staining assay of the Huh7 cells treated with 5 μ M of compounds XAV939 or **3a** for 36 h and together with 200 μ M oleate for 16 h. TD, transmitted light differential interference contrast image. (B) The mRNA expression of various lipogenic and gluconeogenic genes in normal mouse hepatocytes treated with 5 μ M of compound **3a**. Data represents mean \pm S.D. of triplicates.

***In Vivo* Efficacy of Compound **3a** against Diet-Induced Metabolic Disorders in Mice.**

With the promising *in vitro* effects of compound **3a** on metabolism in hepatocytes, we

1
2
3 further studied its efficacy *in vivo* against metabolic disorders using a mouse model.
4
5 Initially, we briefly assessed the pharmacokinetic and physicochemical properties of
6
7 compound **3a**. Compared to the reported parameters for pyrvinium, our new analogue
8
9 showed improved physicochemical and pharmacokinetic properties with an oral
10
11 bioavailability of 21% (pyrvinium has less than 1%). The plasma half-life of compound
12
13 **3a** is 2.8 – 3.3 h, with an oral maximal concentration of 2.2 $\mu\text{g/mL}$ in the plasma after a
14
15 single dose of 10 mg/kg (Table S3). We then proceeded to efficacy studies in the high fat
16
17 diet-fed mouse model. We performed a pilot dose escalation study to determine the optimal
18
19 dose for compound **3a** and to ensure little or no toxicity to the mice (data not shown).
20
21 While we did not observe any noticeable toxicity at up to 200 mg/kg of compound **3a**, we
22
23 found promising efficacy and hepatic improvement at 40 mg/kg so we chose this dose to
24
25 conduct a more comprehensive study in mice. Wild type C57BL/6J mice were fed with a
26
27 high fat diet or normal chow diet for 6 weeks before treatment. The mice were then divided
28
29 into four groups: two were fed normal chow and the other two were fed with the high fat
30
31 diet. Compound **3a** was administered intraperitoneally every 2 days at 40 mg/kg for 11
32
33 weeks, a dose selected based on the pilot dose escalation studies. After 11 weeks of
34
35 treatment, compound **3a** significantly improved glucose tolerance in the high fat diet group
36
37 (Figure 5A-B). The inhibition of Wnt signaling and the improvement of glucose tolerance
38
39 by compound **3a** were confirmed by the decreased hepatic mRNA levels of Wnt target
40
41 genes and those of gluconeogenesis and lipogenesis in the mice fed with the high fat diet,
42
43 respectively (Figure 6A). Of note, the effects of compound **3a** on gene expression were
44
45 insignificant in the mice fed with the normal chow diet, suggesting a selectivity of
46
47 compound **3a** towards metabolic disorders (Figure 6B).
48
49
50
51
52
53
54
55
56
57
58
59
60

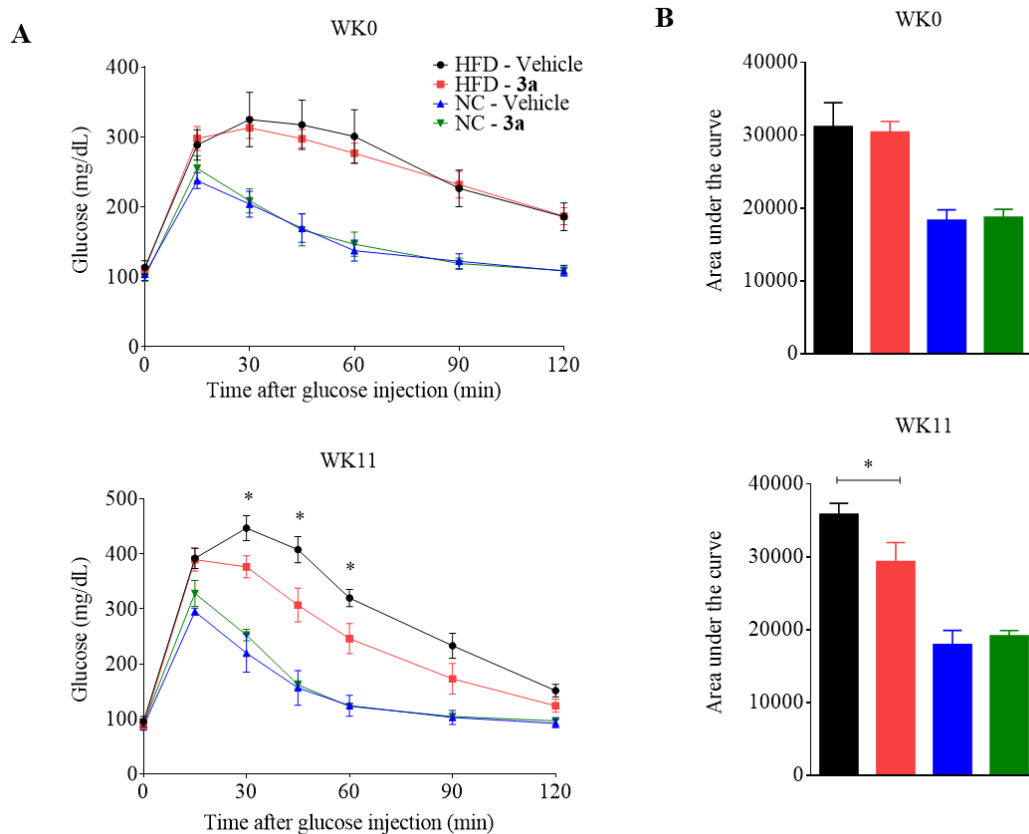


Figure 5. Improvement of glucose tolerance by compound **3a** in *C57BL/6J* mice fed with a high fat diet. (A) Intraperitoneal glucose tolerance test (IPGTT) was carried out on the mice fed with the high fat diet (HFD) and normal chow diet (NC) at the start of treatment (WK0) and after 11 weeks (WK11) of treatment. The mice received intraperitoneal injection of 40 mg/kg compound **3a** or vehicle (corn oil) every two days. (B) The area under the curve (AUC, min*mg/dL) for the IPGTT. Data represents mean \pm SEM, $n = 5$ per group. * $p < 0.05$ as compared to the vehicle group.

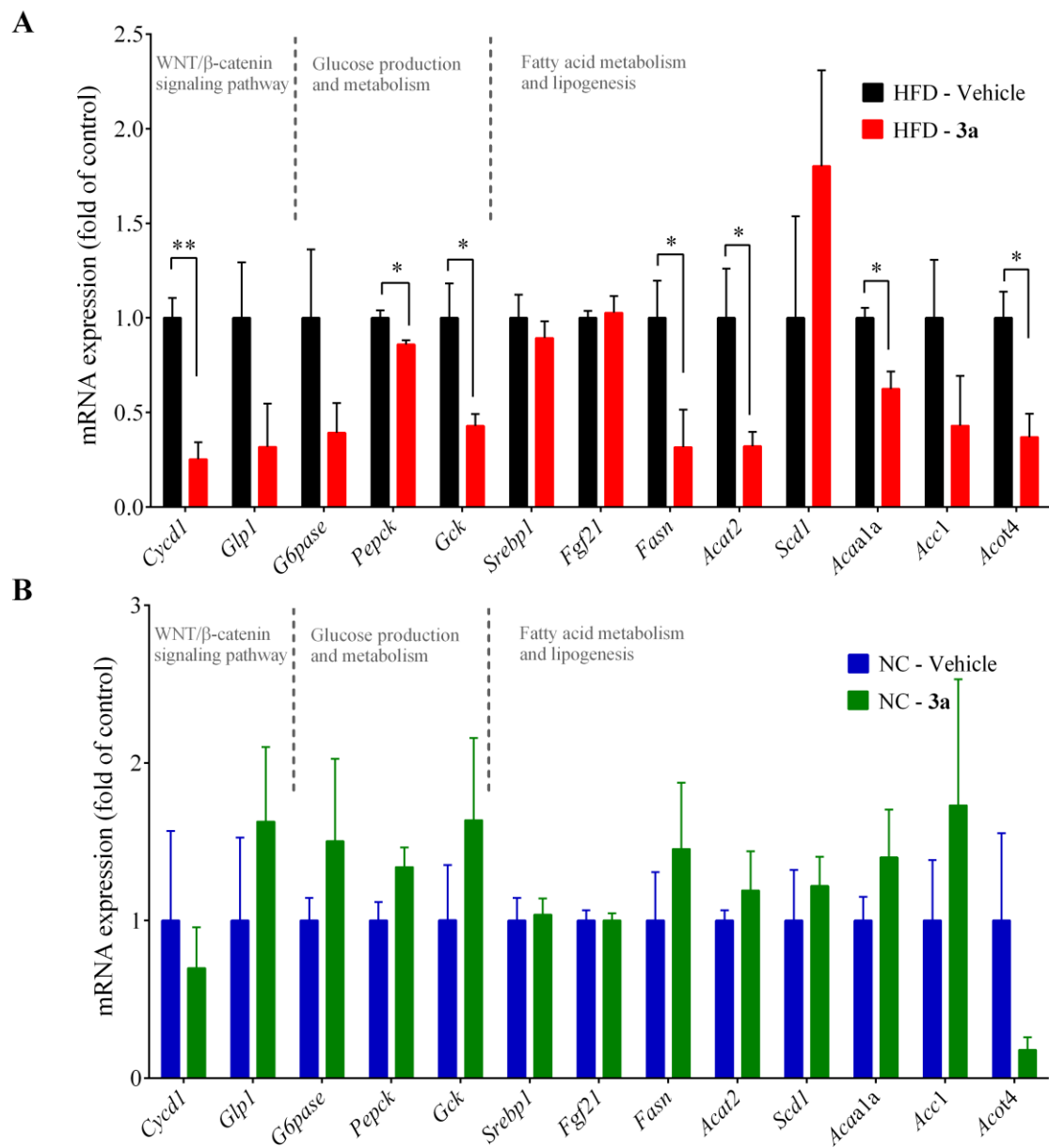


Figure 6. Effects of compound **3a** on the hepatic expression of select Wnt/ β -catenin pathway target genes and those involved in energy metabolism in mice. (A) The mRNA expression of select genes in the mice fed with a high fat diet. (B) The mRNA expression of select genes in the mice fed with normal chow diet. The mice received *i.p.* injection of

1
2
3 40 mg/kg compound **3a** or vehicle (corn oil) every two days for 11 weeks. Data represents
4
5 mean \pm SEM, n = 5 per group. * $p < 0.05$, ** $p < 0.01$.
6
7

8
9 To further assess the efficacy of compound **3a** against the metabolic disorders induced by
10
11 the high fat diet in mice, we conducted additional measurements. The body weight and the
12
13 liver weight adjusted by the body weight were increased in the high fat diet-fed mice.
14
15 However, the increases were suppressed by the treatment of compound **3a**. Of note, the
16
17 treatment caused no effects in the normal chow diet-fed mice (Figure 7). Consistently, in
18
19 our hepatic histological examination, compound **3a** treatment drastically reduced the
20
21 hepatic lipid accumulation induced by the high fat diet. In addition, the hepatic triglyceride
22
23 content and the serum cholesterol level were reduced by the treatment of compound **3a** in
24
25 the high fat diet-fed mice. Importantly, the mice that received compound **3a** treatment did
26
27 not exhibit any significant toxicity as indicated by the blood chemical measurements of
28
29 liver and kidney function and by the histological examination (Table 2, Figure S5). Taken
30
31 together, the effects of compound **3a** were pronounced in the mice with metabolic disorders
32
33 induced by the high fat diet. Inhibition of the Wnt signaling pathway appeared to mediate
34
35 the efficacy of compound **3a** against the metabolic disorders induced by the high fat diet
36
37 because the results phenocopied those seen in genetic knockdown of *Axin*, *Ctnnb1* (β -
38
39 catenin) and *Tcf712* in the mice fed a high fat diet.^{11,46,47}
40
41
42
43
44
45
46
47
48
49
50
51
52
53
54
55
56
57
58
59
60

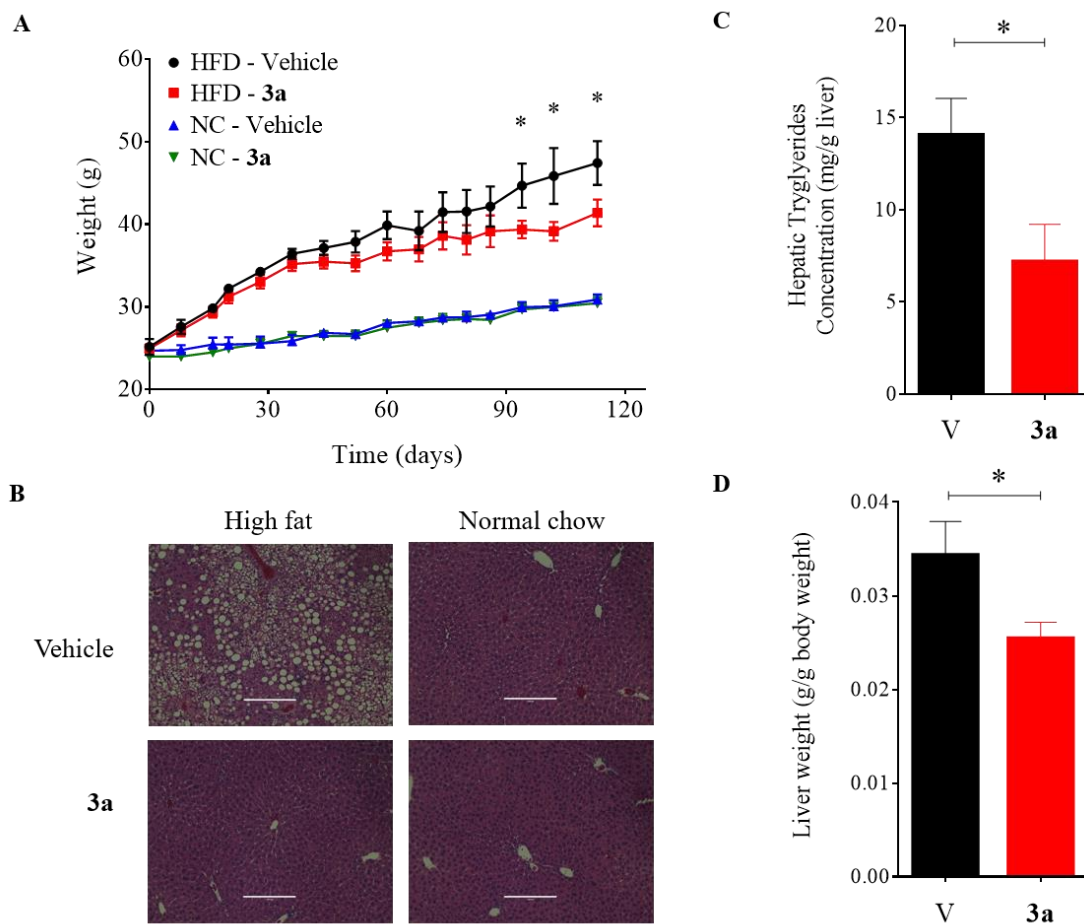


Figure 7. Effects of compound **3a** treatment on body weight gain and hepatic lipid accumulation in *C57BL/6J* mice. (A) Body weight gain in high fat diet and normal chow group mice treated with 40 mg/kg compound **3a** or vehicle (corn oil). (B) Hematoxylin and eosin staining for liver tissue samples. (C) Hepatic triglyceride content and (D) the ratio of liver/body weight in high fat diet-fed mice. The mice received *i.p.* injection of 40 mg/kg compound **3a** or vehicle (corn oil) every two days for 11 weeks. V= vehicle, **3a** = Compound **3a**. * $p < 0.05$.

Table 2. Serum Biochemical Parameters in Mice Received Compound 3a or Vehicle

Physiologic parameter	Unit	High fat diet (n=10)			Normal chow (n=10)		
		vehicle	3a	p-value	vehicle	3a	p-value
ALT	U/L	63.3 ± 26.9	21.0 ± 1.9	NS	20.0 ± 5.1	12.8 ± 1.6	NS
Alkaline Phosphatase	U/L	58.3 ± 3.8	51.0 ± 4.6	NS	66.5 ± 1.8	57.5 ± 1.1	NS
AST	U/L	131 ± 15.6	94.8 ± 17.2	NS	119 ± 28.3	74.5 ± 6.25	NS
Total bilirubin	mg/dL	0.20 ± 0.0	0.20 ± 0.03	NS	0.20 ± 0.0	0.20 ± 0.0	NS
Cholesterol	mg/dL	316 ± 25.0	223 ± 18.1	0.003	183 ± 16.6	194 ± 13.7	NS
Creatinine Jaffe	mg/dL	0.30 ± 0.02	0.20 ± 0.02	NS	0.20 ± 0.01	0.2 ± 0.01	NS
LDH	U/L	469 ± 67	313 ± 40.8	<0.001	324 ± 63.5	190 ± 20.2	<0.001
Triglycerides	mg/dL	93.5 ± 12.1	85.3 ± 7.7	NS	69.0 ± 2.5	55.0 ± 4.8	NS
BUN	mg/dL	17.3 ± 0.5	14.8 ± 0.3	NS	19.0 ± 1.8	21.8 ± 0.5	NS
Uric Acid	mg/dL	6.30 ± 0.5	4.80 ± 0.6	NS	4.00 ± 0.2	3.80 ± 0.3	NS

The mice were fed either a high-fat diet or normal chow diet. Data analysis was performed using ANOVA and Tukey's post-hoc test. The values are expressed as mean ± SE. NS, not significant; ALT, Alanine Aminotransferase; AST, Aspartate aminotransferase; LDH, Lactate dehydrogenase; BUN, Blood urea nitrogen.

CONCLUSION

We have designed, synthesized, and characterized a novel class of triazole-based compounds as novel inhibitors of the Wnt/ β -catenin signaling pathway. One inhibitor of the class, compound **3a**, potently inhibits Wnt/ β -catenin signaling pathway and elicits favorable efficacy against the metabolic disorders induced by high fat diet. Our results have indicated that the new inhibitors stabilized the cellular level of Axin, fortifying the β -catenin destruction complex to attenuate β -catenin cytoplasmic level and suppress the transcription of Wnt/ β -catenin pathway target genes. The identification of direct protein target of compound **3a** is currently underway in our group using biotinylated chemical affinity chromatography, proteomics, and other biochemical methods. Based on the parent scaffold for these new compounds, further modification can be made to generate potent analogues with even improved drug properties that may be applied to the treatment of metabolic disorders, such as fatty liver, diabetes, and obesity, and other diseases, such as cancers, with aberrant regulation of Wnt/ β -catenin pathway.

EXPERIMENTAL SECTION

1. Chemical Analysis. All chemicals were obtained from commercial suppliers and used without further purification. Analytical thin layer chromatography was visualized by ultraviolet light at 256 nm. ^1H NMR spectra were recorded on a Varian (400 MHz) spectrometer. Data are presented as follows: chemical shift (in ppm on the δ scale relative to $\delta = 0.00$ ppm for the protons in tetramethylsilane (TMS), integration, multiplicity (s = singlet, d = doublet, t = triplet, q = quartet, m = multiplet, br = broad), coupling constant (J/Hz). ^{13}C NMR spectra were recorded at 100 MHz, and all chemical shifts values are reported in ppm on the δ scale with an internal reference of $\delta 77.0$ or 39.0 for CDCl_3 or $\text{DMSO-}d_6$, respectively. The purities of title compounds were determined by analytic HPLC, performed on an Agilent 1100 instrument and a reverse-phase column (Waters XTerra RP18, $5\ \mu\text{M}$, $4.6 \times 250\ \text{mm}$). All compounds were eluted with 45% $\text{CH}_3\text{CN}/55\%$ H_2O (0.1% TFA) over 20 min with a detection at 260 nm and a flow rate at 1.0 mL/min. All tested compounds were >95% purity. Yields were not optimized. Compounds **1a-n** and potassium trifluoroborate derivatives were commercially available.

General Procedure A: Synthesis of Compounds 2a-2p. To a mixture of substituted aniline **1a-1n** (20 mmol) in concentrated HCl (8.0 mL) was added a solution of NaNO_2 (1.4 g, 21 mmol) in H_2O (6.0 mL) dropwise at $0\ ^\circ\text{C}$. The mixture was stirred at $0\ ^\circ\text{C}$ for 1 h followed by the addition of a solution of NaN_3 (1.3 g, 20 mmol) in H_2O (6.0 mL) at $0\ ^\circ\text{C}$. The resulting mixture was stirred for another 1 h, extracted with diethyl ether (Et_2O) for three times. The combined organic layers were washed with brine, dried over Na_2SO_4 , and concentrated. To the resulting residue was added ethyl 3-oxobutanoate, or ethyl 3-oxopentanoate, or ethyl 4-methyl-3-oxopentanoate (22 mmol) and a solution of NaOEt

(2.04 g, 30 mmol) in EtOH (120 mL) at room temperature. The mixture was stirred at 80 °C overnight, cooled and concentrated. To the resulting residue was added HCl (1 N, 250 mL) and the resulting precipitate was collected by filtration and washed with water to offer the crude product that was recrystallized from EtOH to give **2a-2p** (25-83%).

5-Methyl-1-(*o*-tolyl)-1*H*-1,2,3-triazole-4-carboxylic acid (2a). The title compound was synthesized according to General Procedure A (55%): ¹H-NMR (400 MHz, DMSO-*d*₆) δ 13.16 (s, 1H), 7.57-7.52 (m, 2H), 7.46-7.44 (m, 2H), 2.32 (s, 3H), 2.00 (s, 3H); ¹³C-NMR (100 MHz, DMSO-*d*₆) δ 163.0, 140.1, 136.5, 135.5, 134.6, 131.7, 131.2, 127.8, 127.6, 17.1, 9.6.

5-Methyl-1-(*m*-tolyl)-1*H*-1,2,3-triazole-4-carboxylic acid (2b). The title compound was synthesized according to General Procedure A (50%): ¹H-NMR (400 MHz, DMSO-*d*₆) δ 13.47 (s, 1H), 7.85 (t, *J* = 8.0 Hz, 1H), 7.78-7.73 (m, 3H), 2.83 (s, 3H), 2.75 (s, 3H); ¹³C-NMR (100 MHz, DMSO-*d*₆) δ 163.0, 140.0, 139.3, 136.9, 135.7, 131.2, 130.0, 126.4, 123.0, 21.3, 10.3.

5-Methyl-1-(*p*-tolyl)-1*H*-1,2,3-triazole-4-carboxylic acid (2c). The title compound was synthesized according to General Procedure A (46%): ¹H-NMR (400 MHz, DMSO-*d*₆) δ 13.08 (s, 1H), 7.42-7.38 (m, 4H), 2.41 (s, 3H), 2.36 (s, 3H); ¹³C-NMR (100 MHz, DMSO-*d*₆) δ 163.1, 140.3, 136.8, 133.3, 130.5, 125.7, 123.2, 21.2, 10.1.

1-(2-Fluorophenyl)-5-methyl-1*H*-1,2,3-triazole-4-carboxylic acid (2d). The title compound was synthesized according to General Procedure A (60%). ¹H-NMR (400 MHz, DMSO-*d*₆) δ 13.24 (s, 1H), 7.74-7.68 (m, 2H), 7.64-7.56 (m, 1H), 7.52-7.45 (m, 1H), 2.40

(s, 3H); ^{13}C -NMR (100 MHz, $\text{DMSO-}d_6$) δ 162.8, 157.5, 155.0, 140.8, 136.7, 133.5, 133.5, 129.5, 126.1, 123.2, 123.0, 117.6, 117.4, 9.5.

1-(2-Bromophenyl)-5-methyl-1H-1,2,3-triazole-4-carboxylic acid (2e). The title compound was synthesized according to General Procedure A (80%): ^1H -NMR (400 MHz, $\text{DMSO-}d_6$) δ 13.26 (s, 1H), 7.98-7.96 (m, 1H), 7.73-7.62 (m, 3H), 2.34 (s, 3H); ^{13}C -NMR (100 MHz, $\text{DMSO-}d_6$) δ 167.6, 145.3, 141.3, 139.3, 138.8, 138.1, 134.9, 134.4, 125.9, 14.4.

1-(2-Cyanophenyl)-5-methyl-1H-1,2,3-triazole-4-carboxylic acid (2f). The title compound was synthesized according to General Procedure A (71%): ^1H -NMR (400 MHz, $\text{DMSO-}d_6$) δ 13.37 (s, 1H), 8.23-8.21 (d, $J = 6.8$ Hz, 1H), 8.05-8.01 (t, $J = 7.2$ Hz), 7.92-7.87 (m, 2H), 2.47 (s, 3H); ^{13}C -NMR (100 MHz, $\text{DMSO-}d_6$) δ 162.7, 140.6, 136.9, 136.8, 135.3, 134.9, 132.0, 128.8, 115.6, 110.5, 9.8.

1-(2-Methoxyphenyl)-5-methyl-1H-1,2,3-triazole-4-carboxylic acid (2g). The title compound was synthesized according to General Procedure A (80%): ^1H -NMR (400 MHz, $\text{DMSO-}d_6$) δ 13.14 (s, 1H), 7.66-7.62 (t, $J = 8.0$ Hz, 1H), 7.49-7.47 (d, $J = 8.0$ Hz, 1H), 7.35-7.33 (d, $J = 8.0$ Hz, 1H), 7.20-7.16 (t, $J = 8.0$ Hz, 1H), 3.80 (s, 3H), 2.31 (s, 3H); ^{13}C -NMR (100 MHz, $\text{DMSO-}d_6$) δ 163.0, 154.1, 140.8, 136.3, 132.7, 128.9, 123.9, 121.3, 113.3, 56.4, 9.5.

1-(2-Carbamoylphenyl)-5-methyl-1H-1,2,3-triazole-4-carboxylic acid (2h). The title compound was synthesized according to General Procedure A (65%): ^1H -NMR (400 MHz, $\text{DMSO-}d_6$) δ 13.10 (s, 1H), 7.93 (s, 1H), 7.70-7.68 (m, 1H), 7.67-7.62 (m, 2H), 7.55-7.52 (m, 1H), 7.38 (s, 1H), 2.38 (s, 3H); ^{13}C -NMR (100 MHz, $\text{DMSO-}d_6$) δ 167.6, 163.2, 140.8, 136.0, 135.9, 131.4, 131.0, 129.1, 128.5, 129.1, 128.5, 128.3, 9.9.

1
2
3 **1-(2-Acetylphenyl)-5-methyl-1H-1,2,3-triazole-4-carboxylic acid (2i).** The title
4
5 compound was synthesized according to General Procedure A (40%): ¹H-NMR (400 MHz,
6 DMSO-*d*₆) δ 8.02-7.99 (m, 1H), 7.77-7.73 (m, 2H), 7.61-7.59 (m, 1H), 2.32 (s, 3H), 2.26
7
8 (s, 3H); ¹³C-NMR (100 MHz, DMSO-*d*₆) δ 199.0, 163.0, 140.7, 136.5, 136.3, 133.3, 132.6,
9
10 131.5, 130.4, 128.8, 29.3, 9.8.
11
12
13
14

15 **5-Methyl-1-(2-morpholinophenyl)-1H-1,2,3-triazole-4-carboxylic acid (2j).** The title
16
17 compound was synthesized according to General Procedure A (83%): ¹H-NMR (400 MHz,
18 DMSO-*d*₆) δ 13.17 (s, 1H), 7.63-7.59 (t, *J* = 8.0 Hz, 1H), 7.44-7.42 (d, *J* = 8.0 Hz, 1H),
19
20 7.33-7.31 (d, *J* = 8.0 Hz, 1H), 7.30-7.26 (t, *J* = 8.0 Hz, 1H), 3.42 (br s, 4H), 2.63 (br s, 4H),
21
22 2.38 (s, 3H); ¹³C-NMR (100 MHz, DMSO-*d*₆) δ 162.9, 148.0, 140.5, 136.7, 132.3, 129.2,
23
24 129.1, 124.0, 120.9, 66.6, 51.4, 10.0.
25
26
27
28
29

30 **1-([1,1'-Biphenyl]-2-yl)-5-methyl-1H-1,2,3-triazole-4-carboxylic acid (2k).** The title
31
32 compound was synthesized according to General Procedure A (65%): ¹H-NMR (400 MHz,
33 DMSO-*d*₆) δ 7.72-7.68 (m, 1H), 7.63-7.61 (m, 2H), 7.53-7.51 (m, 1H), 7.26-7.21 (m, 3H),
34
35 7.02-6.96 (m, 2H), 1.97 (s, 3H); ¹³C-NMR (100 MHz, DMSO-*d*₆) δ 164.2, 140.1, 138.9,
36
37 137.9, 137.5, 133.5, 131.5, 131.4, 129.3, 129.0, 128.8, 128.4, 128.3, 9.5.
38
39
40
41

42 **1-(2,3-Dimethylphenyl)-5-methyl-1H-1,2,3-triazole-4-carboxylic acid (2l).** The title
43
44 compound was synthesized according to General Procedure A (70%): ¹H-NMR (400 MHz,
45 DMSO-*d*₆) δ 13.14 (s, 1H), 7.46-7.45 (m, 1H), 7.36-7.32 (m, 1H), 7.26-7.25 (m, 1H), 2.36
46
47 (s, 3H), 2.30 (s, 3H), 1.81 (s, 3H); ¹³C-NMR (100 MHz, DMSO-*d*₆) δ 167.8, 144.9, 143.9,
48
49 141.2, 139.3, 138.9, 137.0, 131.6, 130.1, 24.9, 18.7, 14.3.
50
51
52
53
54
55
56
57
58
59
60

1
2
3 **1-(2,4-Dimethylphenyl)-5-methyl-1H-1,2,3-triazole-4-carboxylic acid (2m)**. The title
4
5 compound was synthesized according to General Procedure A (73%): ¹H-NMR (400 MHz,
6 DMSO-*d*₆) δ 13.01 (s, 1H), 7.28-7.24 (m, 2H), 7.20-7.18 (m, 1H), 2.34 (s, 3H), 2.26 (s,
7 3H), 1.88 (s, 3H); ¹³C-NMR (100 MHz, DMSO-*d*₆) δ 163.0, 140.9, 140.1, 136.4, 135.1,
8 132.2, 132.1, 128.0, 127.5, 21.1, 17.0, 9.6.
9
10
11
12
13
14

15 **5-Methyl-1-(naphthalen-1-yl)-1H-1,2,3-triazole-4-carboxylic acid (2n)**. The title
16
17 compound was synthesized according to General Procedure A (72%): ¹H-NMR (400 MHz,
18 DMSO-*d*₆) δ 13.15 (s, 1H), 8.27-8.25 (d, *J* = 8.0 Hz, 1H), 8.16-8.14 (d, *J* = 8.0 Hz, 1H),
19 7.80-7.30 (m, 2H), 7.69-7.65 (t, *J* = 8.0 Hz, 1H), 7.62-7.58 (t, *J* = 8.0 Hz, 1H), 7.14-7.12
20 (d, *J* = 8.0 Hz, 1H), 2.31 (s, 3H); ¹³C-NMR (100 MHz, DMSO-*d*₆) δ 163.0, 141.1, 136.7,
21 134.1, 131.5, 129.2, 128.9, 128.8, 127.9, 127.7, 126.2, 126.0, 122.0, 9.7.
22
23
24
25
26
27
28
29

30 **5-Ethyl-1-(2-fluorophenyl)-1H-1,2,3-triazole-4-carboxylic acid (2o)**. The title
31
32 compound was synthesized according to General Procedure A (80%): ¹H-NMR (400 MHz,
33 DMSO-*d*₆) δ 13.31 (s, 1H), 7.77-7.74 (m, 2H), 7.64-7.59 (t, *J* = 8.8 Hz, 1H), 7.52-7.48 (t,
34 *J* = 8.0 Hz, 1H), 2.84-2.78 (q, *J* = 7.2 Hz, 2H), 1.02-0.98 (t, *J* = 7.2 Hz, 3H); ¹³C-NMR
35 (100 MHz, DMSO-*d*₆) δ 167.4, 162.6, 160.1, 150.5, 140.9, 138.6, 138.5, 134.6, 130.9,
36 130.8, 122.3, 122.1, 21.6, 17.6.
37
38
39
40
41
42
43

44 **1-(2-Fluorophenyl)-5-isopropyl-1H-1,2,3-triazole-4-carboxylic acid (2p)**. The title
45
46 compound was synthesized according to General Procedure A (25%): ¹H-NMR (400 MHz,
47 DMSO-*d*₆) δ 13.01 (s, 1H), 7.77-7.74 (m, 2H), 7.64-7.60 (t, *J* = 8.0 Hz, 1H), 7.52-7.48 (t,
48 *J* = 8.0 Hz, 1H), 3.24-3.20 (m, 1H), 1.23-1.21 (d, *J* = 6.8 Hz, 6H); ¹³C-NMR (100 MHz,
49 DMSO-*d*₆) δ 167.6, 162.8, 160.3, 153.5, 140.6, 138.7, 138.6, 135.0, 130.8, 122.2, 122.0,
50 29.5, 24.6.
51
52
53
54
55
56
57
58
59
60

General Procedure B: Synthesis of Compounds 3a-3r. To a solution of 2-aminoquinoline or naphthalen-2-amine or 6-bromoquinolin-2-amine (0.5 mmol) and **2a-2p** (0.675 mmol) in DCE (2 mL) was added PyCIU (0.775 mmol) and DIPEA (2.33 mmol). The mixture was stirred at 80 °C overnight, then cooled and concentrated. To the resulting residue was added ethyl acetate (30 mL), and the mixture was washed with brine, dried over Na₂SO₄ and concentrated. The crude material was purified by column chromatography (hexane/AcOEt, v/v = 4/1 to 2/1) to give products **3a-3r** (47-69%).

5-Methyl-N-(quinolin-2-yl)-1-(o-tolyl)-1H-1,2,3-triazole-4-carboxamide (3a). The title compound was synthesized according to General Procedure B (60%, a white solid): ¹H-NMR (400 MHz, DMSO-*d*₆) δ 10.22 (s, 1H), 8.49-8.47 (d, *J* = 8.8 Hz, 1H), 8.42-8.40 (d, *J* = 8.8 Hz, 1H), 8.00-7.98 (d, *J* = 8.0 Hz, 1H), 7.91-7.89 (d, *J* = 8.0 Hz, 1H), 7.69 (t, *J* = 8.0 Hz, 1H), 7.61-7.56 (m, 3H), 7.51-7.50 (m, 2H), 2.45 (s, 3H), 2.04 (s, 3H); ¹³C-NMR (100 MHz, DMSO-*d*₆) δ 160.0, 150.8, 146.8, 139.5, 139.1, 137.6, 135.5, 134.4, 131.8, 131.4, 130.7, 128.3, 127.8, 127.7, 127.7, 126.4, 125.8, 114.7, 17.2, 9.4. HRMS (ESI): *m/z* [M + H]⁺ calcd for C₂₀H₁₈N₅O, 344.1511, found, 344.1510. HPLC: *t*_R = 8.75 min, 98.2%.

5-Methyl-N-(quinolin-2-yl)-1-(m-tolyl)-1H-1,2,3-triazole-4-carboxamide (3b). The title compound was synthesized according to General Procedure B (65%, a white solid): ¹H-NMR (400 MHz, CDCl₃) δ 9.92 (s, 1H), 8.57 (d, *J* = 8.0 Hz, 1H), 8.22 (d, *J* = 8.0 Hz, 1H), 7.92 (d, *J* = 8.0 Hz, 1H), 7.81 (d, *J* = 8.0 Hz, 1H), 7.70 (t, *J* = 7.2, 7.6 Hz, 1H), 7.47 (d, *J* = 7.2 Hz, 2H), 7.38 (d, *J* = 8.0 Hz, 1H), 7.33 (s, 1H), 7.27 (d, *J* = 5.6 Hz, 1H), 2.71 (s, 3H), 2.48 (s, 3H); ¹³C-NMR (100 MHz, CDCl₃) δ 160.0, 150.6, 146.9, 140.1, 138.4, 138.1, 137.9, 135.3, 130.9, 129.9, 129.4, 127.8, 127.5, 126.4, 125.9, 125.1, 122.2, 114.2,

21.3, 9.9; HRMS (ESI): calcd. for C₂₀H₁₈N₅O [M + H]⁺ 344.1511, found 344.1508. HPLC: *t*_R = 6.51 min, 100%.

5-Methyl-*N*-(quinolin-2-yl)-1-(*p*-tolyl)-1*H*-1,2,3-triazole-4-carboxamide (3c). The title compound was synthesized according to General Procedure B (68%, a white solid): ¹H-NMR (400 MHz, CDCl₃) δ 9.91 (s, 1H), 8.55 (d, *J* = 8.0 Hz, 1H), 8.20 (d, *J* = 8.0 Hz, 1H), 7.90 (d, *J* = 8.0 Hz, 1H), 7.79 (d, *J* = 8.0 Hz, 1H), 7.68 (t, *J* = 7.6, 8.0 Hz, 1H), 7.45 (t, *J* = 6.8, 8.0 Hz, 1H), 7.43-7.35 (m, 4H), 2.68 (s, 3H), 2.46 (s, 3H); ¹³C-NMR (100 MHz, CDCl₃) δ 160.0, 150.6, 146.9, 140.4, 138.4, 138.1, 137.9, 132.9, 130.2, 129.9, 127.8, 127.5, 126.4, 125.1, 125.0, 114.2, 21.3, 9.9; HRMS (ESI): *m/z* [M + H]⁺ calcd for C₂₀H₁₈N₅O, 344.1511; found, 344.1511. HPLC: *t*_R = 6.40 min, 99.9%.

1-(2-Fluorophenyl)-5-methyl-*N*-(quinolin-2-yl)-1*H*-1,2,3-triazole-4-carboxamide

(3d). The title compound was synthesized according to General Procedure B (50%, a white solid): ¹H-NMR (400 MHz, DMSO-*d*₆) δ 10.25 (s, 1H), 8.46-8.44 (m, 2H), 7.97-7.54 (m, 9H), 2.52 (s, 3H); ¹³C-NMR (100 MHz, DMSO-*d*₆) δ 159.8, 157.5, 155.0, 150.8, 146.8, 140.2, 139.1, 137.7, 133.7, 130.6, 129.5, 128.2, 127.7, 126.4, 126.2, 125.8, 123.0, 117.7, 117.5, 114.7, 9.3. HRMS (ESI): *m/z* [M + H]⁺ calcd for C₁₉H₁₅FN₅O, 348.1261; found, 348.1252. HPLC: *t*_R = 9.53 min, 99.9%.

1-(2-Bromophenyl)-5-methyl-*N*-(quinolin-2-yl)-1*H*-1,2,3-triazole-4-carboxamide

(3e). The title compound was synthesized according to General Procedure B (68%, a white solid): ¹H-NMR (400 MHz, DMSO-*d*₆) δ 10.26 (s, 1H), 8.48-8.46 (d, *J* = 8.0 Hz, 1H), 8.41-8.39 (d, *J* = 8.0 Hz, 1H), 8.02-8.99 (t, *J* = 8.8 Hz, 2H), 7.91-7.89 (d, *J* = 8.0 Hz, 1H), 7.77-7.67 (m, 4H), 7.57-7.53 (d, *J* = 8.0 Hz, 1H), 2.46 (s, 3H); ¹³C-NMR (100 MHz, DMSO-*d*₆) δ 164.6, 155.5, 151.6, 144.7, 143.9, 142.3, 139.2, 138.9, 138.3, 135.4, 135.0, 134.5, 133.0,

1
2
3 132.5, 131.2, 130.6, 125.9, 119.6, 14.2. HRMS (ESI): m/z $[M + H]^+$ calcd for
4 $C_{19}H_{15}BrN_5O_2$, 408.0460; found, 408.0458. HPLC: $t_R = 8.21$ min, 99.9%.

7
8
9 **1-(2-Cyanophenyl)-5-methyl-N-(quinolin-2-yl)-1H-1,2,3-triazole-4-carboxamide (3f).**

10 The title compound was synthesized according to General Procedure B (57%, a white
11 solid): 1H -NMR (400 MHz, DMSO- d_6) δ 10.35 (s, 1H), 8.49-8.46 (d, $J = 8.8$ Hz, 1H), 8.40-
12 8.38 (d, $J = 8.8$ Hz, 1H), 8.27-8.25 (d, $J = 8.0$ Hz, 1H), 8.08-8.04 (t, $J = 8.0$ Hz, 1H), 7.99-
13 7.96 (t, 2H), 7.94-7.90 (t, $J = 8.0$ Hz, 2H), 7.79-7.75 (t, $J = 8.0$ Hz, 1H), 7.57-7.53 (t, $J =$
14 8.0 Hz, 1H), 2.60 (s, 3H); ^{13}C -NMR (100 MHz, DMSO- d_6) δ 159.7, 150.8, 146.8, 140.1,
15 139.1, 138.0, 136.6, 135.4, 135.1, 132.1, 130.7, 128.8, 128.3, 127.8, 126.4, 125.8, 115.6,
16 114.9, 110.5, 9.6. HRMS (ESI): m/z $[M + H]^+$ calcd for $C_{20}H_{15}N_6O$, 355.1307; found
17 355.1304. HPLC: $t_R = 7.45$ min, 99.8%.

18
19
20
21
22
23
24
25
26
27
28
29
30 **1-(2-Methoxyphenyl)-5-methyl-N-(quinolin-2-yl)-1H-1,2,3-triazole-4-carboxamide**

31 **(3g).** The title compound was synthesized according to General Procedure B (48%, a white
32 solid): 1H -NMR (400 MHz, DMSO- d_6) δ 10.28 (s, 1H), 8.61-8.51 (m, 2H), 8.09 (m, 1H),
33 8.01 (m, 1H), 7.88 (m, 1H), 7.78 (m, 1H), 7.66 (m, 2H), 7.52-7.47 (m, 1H), 7.35-7.32 (m,
34 1H), 3.97-3.94 (q, $J = 4$ Hz, 3H), 2.56-2.53 (q, $J = 4$ Hz, 3H); ^{13}C -NMR (100 MHz, DMSO-
35 d_6) δ 160.0, 154.1, 150.9, 146.2, 140.2, 139.1, 137.3, 132.9, 130.6, 128.9, 128.2, 127.7,
36 126.4, 125.7, 123.7, 121.4, 114.7, 113.4, 56.5, 9.4. HRMS (ESI): m/z $[M + H]^+$ calcd for
37 $C_{20}H_{18}N_5O_2$, 360.1460; found, 360.1460. HPLC: $t_R = 8.88$ min, 99.8%.

38
39
40
41
42
43
44
45
46
47
48
49 **1-(2-Carbamoylphenyl)-5-methyl-N-(quinolin-2-yl)-1H-1,2,3-triazole-4-carboxamide**

50 **(3h).** The title compound was synthesized according to General Procedure B (49%, a pale
51 yellow solid): 1H -NMR (400 MHz, DMSO- d_6) δ 10.13 (s, 1H), 8.48-8.46 (d, $J = 8.8$ Hz,
52 1H), 8.42-8.39 (d, $J = 8.8$ Hz, 1H), 8.06 (s, 1H), 7.99-7.97 (d, $J = 8.0$ Hz, 1H), 7.90-7.88
53 54 55 56 57 58 59 60

(d, $J = 8.0$ Hz, 1H), 7.80-7.74 (m, 4H), 7.68-7.66 (m, 1H), 7.57-7.53 (t, $J = 8.0$ Hz, 1H), 7.49 (s, 1H), 2.50 (s, 3H); ^{13}C -NMR (100 MHz, DMSO- d_6) δ 172.3, 164.8, 155.6, 151.6, 145.1, 143.9, 141.7, 139.7, 137.6, 136.2, 135.9, 135.4, 133.9, 133.3, 133.0, 132.5, 131.2, 130.5, 119.4, 14.4. HRMS (ESI): m/z $[\text{M} + \text{H}]^+$ calcd for $\text{C}_{20}\text{H}_{17}\text{N}_6\text{O}_2$, 373.1413; found, 373.1413. HPLC: $t_{\text{R}} = 2.72$ min, 95.0%.

1-(2-Acetylphenyl)-5-methyl-N-(quinolin-2-yl)-1H-1,2,3-triazole-4-carboxamide (3i).

The title compound was synthesized according to General Procedure B (48%, a brown solid): ^1H -NMR (400 MHz, DMSO- d_6) δ 10.37 (s, 1H), 8.65-8.63 (d, $J = 8.8$ Hz, 1H), 8.58-8.56 (d, $J = 8.8$ Hz, 1H), 8.30-8.28 (d, $J = 7.2$ Hz, 1H), 8.16-8.14 (d, $J = 8.0$ Hz, 1H), 8.07-8.01 (m, 3H), 7.95-7.89 (m, 2H), 7.74-7.70 (t, $J = 7.2$ Hz, 1H), 2.67 (s, 6H); ^{13}C -NMR (100 MHz, DMSO- d_6) δ 203.7, 164.7, 155.6, 151.6, 144.9, 143.9, 142.3, 140.9, 138.2, 137.1, 136.4, 135.4, 133.6, 133.0, 132.5, 131.2, 130.5, 119.5, 34.1, 14.3. HRMS (ESI): m/z $[\text{M} + \text{H}]^+$ calcd for $\text{C}_{21}\text{H}_{18}\text{N}_5\text{O}_2$, 372.1460; found, 372.1455. HPLC: $t_{\text{R}} = 7.39$ min, 99.2%.

5-Methyl-1-(2-morpholinophenyl)-N-(quinolin-2-yl)-1H-1,2,3-triazole-4-

carboxamide (3j). The title compound was synthesized according to General Procedure B (48%, a white solid): ^1H -NMR (400 MHz, DMSO- d_6) δ 10.20 (s, 1H), 8.48-8.46 (d, $J = 8.8$ Hz, 1H), 8.43-8.40 (d, $J = 8.8$ Hz, 1H), 7.99-7.97 (d, $J = 8.4$ Hz, 1H), 7.90-7.88 (d, $J = 8.4$ Hz, 1H), 7.78-7.74 (t, $J = 8.0$ Hz, 1H), 7.66-7.62 (t, $J = 8.0$ Hz, 1H), 7.57-7.53 (t, $J = 8.0$ Hz, 1H), 7.50-7.48 (d, $J = 8.0$ Hz, 1H), 7.37-7.33 (t, $J = 8.0$ Hz, 1H), 7.31-7.29 (d, $J = 8.0$ Hz, 1H), 3.45 (br s, 4H), 2.67 (br s, 4H), 2.50 (s, 3H); ^{13}C -NMR (100 MHz, DMSO- d_6) δ 159.9, 150.8, 146.8, 139.8, 139.1, 137.8, 132.4, 130.6, 129.3, 129.0, 128.3, 127.7, 126.4, 125.7, 124.1, 121.0, 114.7, 66.6, 51.4, 9.7. HRMS (ESI): m/z $[\text{M} + \text{H}]^+$ calcd for $\text{C}_{23}\text{H}_{23}\text{N}_6\text{O}_2$, 415.1882; found, 415.1873. HPLC: $t_{\text{R}} = 10.48$ min, 99.6%.

1-([1,1'-Biphenyl]-2-yl)-5-methyl-N-(quinolin-2-yl)-1H-1,2,3-triazole-4-carboxamide

(**3k**). The title compound was synthesized according to General Procedure B (58%, a white solid): ¹H-NMR (400 MHz, DMSO-*d*₆) δ 10.11 (s, 1H), 8.45-8.43 (d, *J* = 8.0 Hz, 1H), 8.33-8.31 (d, *J* = 8.0 Hz, 1H), 7.98-7.96 (d, *J* = 8.0 Hz, 1H), 7.89-7.87 (d, *J* = 8.0 Hz, 1H), 7.81-7.69 (m, 5H), 7.56-7.52 (t, *J* = 7.2 Hz, 1H), 7.34-7.32 (m, 3H), 7.09-7.07 (m, 2H), 2.16 (s, 3H); ¹³C-NMR (100 MHz, DMSO-*d*₆) δ 159.7, 150.7, 146.8, 139.6, 139.1, 137.4, 137.2, 132.8, 131.9, 131.5, 130.6, 129.5, 129.2, 128.7, 128.5, 128.2, 127.7, 126.4, 125.8, 114.7, 9.28. HRMS (ESI): *m/z* [M + H]⁺ calcd for C₂₅H₂₀N₅O, 406.1668; found, 406.1665. HPLC: *t*_R = 11.17 min, 99.9%.

1-(2,3-Dimethylphenyl)-5-methyl-N-(quinolin-2-yl)-1H-1,2,3-triazole-4-carboxamide

(**3l**). The title compound was synthesized according to General Procedure B (67%, a white solid): ¹H-NMR (400 MHz, CDCl₃) δ 9.95 (s, 1H), 8.57-8.55 (d, *J* = 8.4 Hz, 1H), 8.23-8.21 (d, *J* = 8.4 Hz, 1H), 7.93-7.91 (d, *J* = 8.8 Hz, 1H), 7.81-7.79 (d, *J* = 8.4 Hz, 1H), 7.71-7.67 (t, *J* = 8.0 Hz, 1H), 7.49-7.45 (t, *J* = 7.2 Hz, 1H), 7.40-7.38 (d, *J* = 7.2 Hz, 1H), 7.31-7.27 (t, *J* = 8.0 Hz, 1H), 7.12-7.10 (d, *J* = 8.0 Hz, 1H), 2.50 (s, 3H), 2.39 (s, 3H), 1.91 (s, 3H); ¹³C-NMR (100 MHz, CDCl₃) δ 160.1, 150.6, 146.9, 139.1, 139.0, 138.4, 137.7, 134.3, 134.0, 132.2, 129.9, 127.8, 127.5, 126.5, 126.4, 125.1, 124.8, 114.2, 20.3, 14.0, 9.3. HRMS (ESI): *m/z* [M + H]⁺ calcd for C₂₁H₂₀N₅O, 358.1668; found, 358.1670. HPLC: *t*_R = 11.23 min, 99.9%.

1-(2,4-Dimethylphenyl)-5-methyl-N-(quinolin-2-yl)-1H-1,2,3-triazole-4-carboxamide

(**3m**). The title compound was synthesized according to General Procedure B (69%, a white solid): ¹H-NMR (400 MHz, CDCl₃) δ 9.94 (s, 1H), 8.57-8.55 (d, *J* = 8.8 Hz, 1H), 8.23-8.21 (d, *J* = 8.8 Hz, 1H), 7.93-7.91 (d, *J* = 8.0 Hz, 1H), 7.82-7.80 (d, *J* = 8.0 Hz, 1H), 7.71-

1
2
3 7.67 (t, $J = 8.0$ Hz, 1H), 7.49-7.45 (t, $J = 8.0$ Hz, 1H), 7.26-7.24 (d, $J = 8.0$ Hz, 1H), 7.20-
4 7.18 (d, $J = 8.0$ Hz, 1H), 7.15-7.13 (d, $J = 8.0$ Hz, 1H), 2.51 (s, 3H), 2.44 (s, 3H), 2.03 (s,
5 3H); ^{13}C -NMR (100 MHz, CDCl_3) δ 160.1, 150.6, 141.1, 138.9, 138.4, 137.7, 135.1, 132.1,
6 131.7, 129.9, 127.8, 127.7, 127.5, 126.9, 126.4, 125.1, 114.2, 21.5, 17.1, 9.3. HRMS (ESI):
7 m/z $[\text{M} + \text{H}]^+$ calcd for $\text{C}_{21}\text{H}_{20}\text{N}_5\text{O}$ 358.1668, found 358.1661. HPLC: $t_{\text{R}} = 17.12$ min,
8 99.9%.
9
10
11
12
13
14
15
16

17 **5-Methyl-1-(naphthalen-1-yl)-*N*-(quinolin-2-yl)-1*H*-1,2,3-triazole-4-carboxamide**

18 **(3n)**. The title compound was synthesized according to General Procedure B (47%, a white
19 solid): ^1H -NMR (400 MHz, $\text{DMSO}-d_6$) δ 10.56 (s, 1H), 8.76-8.69 (m, 2H), 8.58-8.56 (d, J
20 = 8.0 Hz, 1H), 8.46-8.44 (d, $J = 8.0$ Hz, 1H), 8.26-8.24 (d, $J = 8.0$ Hz, 1H), 8.19-8.17 (d, J
21 = 8.0 Hz, 1H), 8.10 (s, 1H), 8.07-8.10 (m, 2H), 7.97-7.95 (m, 1H), 7.92-7.89 (t, $J = 6.4$ Hz,
22 1H), 7.82 (t, $J = 6.4$ Hz, 1H), 7.49-7.47 (d, $J = 8.0$ Hz, 1H), 2.67 (s, 3H); ^{13}C -NMR (100
23 MHz, $\text{DMSO}-d_6$) δ 160.0, 150.9, 146.8, 140.4, 139.2, 137.8, 134.1, 131.7, 131.4, 130.7,
24 129.2, 128.9, 128.8, 128.3, 127.8, 127.7, 126.4, 126.3, 126.0, 125.8, 122.1, 114.7, 9.5.
25 HRMS (ESI): m/z $[\text{M} + \text{H}]^+$ calcd for $\text{C}_{23}\text{H}_{18}\text{N}_5\text{O}$, 380.1511; found, 380.1512. HPLC: $t_{\text{R}} =$
26 9.54 min, 97.4 %.
27
28
29
30
31
32
33
34
35
36
37
38
39
40

41 **5-Ethyl-1-(2-fluorophenyl)-*N*-(quinolin-2-yl)-1*H*-1,2,3-triazole-4-carboxamide (3o)**

42 The title compound was synthesized according to General Procedure B (60%, a white
43 solid): ^1H -NMR (400 MHz, $\text{DMSO}-d_6$) δ 10.28 (s, 1H), 8.49-8.46 (d, $J = 8.8$ Hz, 1H), 8.42-
44 8.40 (d, $J = 8.8$ Hz, 1H), 8.00-7.98 (d, $J = 8.8$ Hz, 1H), 7.91-7.89 (d, $J = 8.8$ Hz, 1H), 7.84-
45 7.75 (m, 3H), 7.69-7.65 (t, $J = 8.0$ Hz, 1H), 7.57-7.53 (m, 2H), 2.96-2.91 (q, $J = 7.2$ Hz,
46 2H), 1.11-1.08 (t, $J = 7.2$ Hz, 3H); ^{13}C -NMR (100 MHz, $\text{DMSO}-d_6$) δ 164.4, 162.6, 160.1,
47 155.6, 151.6, 149.9, 143.9, 142.1, 138.8, 138.7, 135.4, 134.6, 133.0, 132.5, 131.2, 131.0,
48
49
50
51
52
53
54
55
56
57
58
59
60

1
2
3 130.9, 130.5, 122.4, 122.2, 119.5, 21.6, 17.5. HRMS (ESI): m/z $[M + H]^+$ calcd for
4 $C_{20}H_{17}FN_5O$, 362.1417; found, 362.1415. HPLC: t_R = 14.04 min, 99.7%.
5
6

7
8 **1-(2-Fluorophenyl)-5-isopropyl-N-(quinolin-2-yl)-1H-1,2,3-triazole-4-carboxamide**
9

10 **(3p)**. The title compound was synthesized according to General Procedure B (69%, a white
11 solid): 1H -NMR (400 MHz, $DMSO-d_6$) δ 10.34 (s, 1H), 8.49-8.47 (d, J = 8.8 Hz, 1H), 8.43-
12 8.41 (d, J = 8.8 Hz, 1H), 8.00-7.98 (d, J = 8.8 Hz, 1H), 7.91-7.89 (d, J = 8.8 Hz, 1H), 7.84-
13 7.75 (m, 3H), 7.69-7.65 (t, J = 8.0 Hz, 1H), 7.57-7.53 (m, 2H), 3.24-3.20 (m, 1H), 1.34-
14 1.32 (d, J = 7.2 Hz, 6H); ^{13}C -NMR (100 MHz, $DMSO-d_6$) δ 164.3, 162.8, 160.3, 155.6,
15 153.1, 151.6, 143.9, 142.1, 138.9, 138.8, 135.4, 134.9, 133.0, 132.5, 131.2, 131.0, 130.5,
16 128.4, 128.3, 122.3, 122.1, 119.5, 29.7, 24.8. HRMS (ESI): m/z $[M + H]^+$ calcd for
17 $C_{21}H_{19}FN_5O$, 376.1574; found, 376.1581. HPLC: t_R = 10.69 min, 99.0%.
18
19
20
21
22
23
24
25
26
27
28
29

30 **5-Methyl-N-(naphthalen-2-yl)-1-(o-tolyl)-1H-1,2,3-triazole-4-carboxamide (3q)**. The
31 title compound was synthesized according to General Procedure B (57%, a white solid):
32
33

34 1H -NMR (400 MHz, $CDCl_3$) δ 9.28 (s, 1H), 8.47 (s, 1H), 7.87-7.81 (m, 3H), 7.67-7.64 (dd,
35 J_1 = 1.6 Hz, J_2 = 8.8 Hz, 1H), 7.53-7.39 (m, 5H), 7.26 (s, 1H), 2.53 (s, 3H), 2.09 (s, 3H);
36 ^{13}C -NMR (100 MHz, $CDCl_3$) δ 159.4, 138.4, 138.1, 135.5, 135.2, 134.3, 133.9, 131.5,
37 130.8, 130.7, 128.8, 127.7, 127.6, 127.2, 127.1, 126.5, 125.0, 119.8, 116.4, 17.2, 9.2.
38 HRMS (ESI): m/z $[M + H]^+$ calcd for $C_{21}H_{19}N_4O$, 343.1559; found, 343.1561. HPLC: t_R =
39 11.64 min, 98.6%.
40
41
42
43
44
45
46
47
48

49 **N-(6-Bromoquinolin-2-yl)-5-methyl-1-(o-tolyl)-1H-1,2,3-triazole-4-carboxamide (3r)**.
50

51 The title compound was synthesized according to General Procedure B (60%, a white
52 solid): 1H -NMR (400 MHz, $CDCl_3$) δ 9.98 (s, 1H), 8.59 (d, J = 8.4 Hz, 1H), 8.13 (d, J =
53 8.0 Hz, 1H), 7.95 (s, 1H), 7.80-7.75 (m, 2H), 7.51-7.49 (m, 1H), 7.45-7.40 (m, 2H), 7.26
54
55
56
57
58
59
60

(s, 1H), 2.51 (s, 3H), 2.08 (s, 3H); ¹³C-NMR (100 MHz, CDCl₃) δ 160.0, 150.8, 139.0, 137.8, 135.5, 134.2, 133.4, 131.5, 130.9, 129.5, 129.3, 127.1, 118.7, 115.0, 17.2, 9.3; HRMS (ESI): m/z [M + H]⁺ calcd for C₂₀H₁₇BrN₅O, 422.0616; found, 422.0621. HPLC: *t*_R = 8.14 min, 98.2%.

General Procedure C: Synthesis of Compounds 3s-3u. In a conical shaped microwave vial was added **3r** (0.169 mmol), potassium trifluoroborate derivatives (0.338 mmol), 2-dicyclohexylphosphino-2',4',6'-triisopropylbiphenyl (XPhos, 0.034 mmol), cesium carbonate (0.507 mmol), and palladium (II) acetate (0.017 mmol), THF (0.5 mL) and water (0.05 mL). The reaction mixture was sealed and stirred at room temperature for 10 min. Once a clear solution was obtained, the vial was heated to 80 °C for 15 min followed by 145 °C for 45 min. After cooling, the reaction mixture was diluted with DCM and dried over Na₂SO₄. The solution was filtered, concentrated and purified by column chromatography (5-15% MeOH in DCM) to give compounds **3s-3u** (55-73%).

5-Methyl-N-(6-(morpholinomethyl)quinolin-2-yl)-1-(*o*-tolyl)-1*H*-1,2,3-triazole-4-carboxamide (3s). The title compound was synthesized according to General Procedure C (73%, a white solid): ¹H-NMR (400 MHz, CDCl₃) δ 9.91 (s, 1H), 8.54 (d, *J* = 8.8 Hz, 1H), 8.17 (d, *J* = 8.8 Hz, 1H), 7.86 (d, *J* = 7.6 Hz, 1H), 7.71-7.69 (m, 2H), 7.49-7.47 (m, 1H), 7.43-7.39 (m, 2H), 7.25 (d, *J* = 7.2 Hz, 1H), 3.74-3.67 (m, 6H), 2.50-2.51 (m, 7H), 2.06 (s, 3H); ¹³C-NMR (100 MHz, CDCl₃) δ 160.0, 150.5, 146.4, 138.8, 138.2, 137.7, 135.5, 134.2, 131.5, 131.4, 130.9, 127.8, 127.4, 127.1, 126.1, 114.3, 66.8, 63.1, 53.6, 17.2, 9.3; HRMS (ESI): m/z [M + H]⁺ calcd for C₂₅H₂₇N₆O₂, 443.2195; found, 443.2189. HPLC: *t*_R = 1.96 min, 97.2%.

1
2
3 **5-Methyl-N-(6-(piperidin-1-ylmethyl)quinolin-2-yl)-1-(*o*-tolyl)-1*H*-1,2,3-triazole-4-**
4 **carboxamide (3t).** The title compound was synthesized according to General Procedure C
5
6 (55%, a white solid): ¹H-NMR (400 MHz, CDCl₃) δ 9.89 (s, 1H), 8.51 (d, *J* = 8.0 Hz, 1H),
7
8 8.15 (d, *J* = 8.4 Hz, 1H), 7.83 (d, *J* = 8.4 Hz, 1H), 7.68-7.66 (m, 2H), 7.47-7.46 (m, 1H),
9
10 7.42-7.36 (m, 2H), 7.24 (d, *J* = 7.6 Hz, 1H), 3.61 (s, 2H), 2.49 (s, 3H), 2.41-2.40 (m, 4H),
11
12 2.05 (s, 3H), 1.58-1.57 (m, 4H), 1.43-1.41 (m, 2H); ¹³C-NMR (100 MHz, CDCl₃) δ 159.9,
13
14 150.3, 146.3, 138.8, 138.2, 137.8, 135.8, 135.5, 134.3, 131.7, 131.5, 130.8, 127.5, 127.2,
15
16 127.1, 126.1, 114.1, 63.6, 54.6, 25.9, 24.3, 17.2, 9.3; HRMS (ESI): *m/z* [M + H]⁺ calcd for
17
18 C₂₆H₂₉N₆O, 441.2403; found, 441.2417. HPLC: *t*_R = 2.05 min, 100%.

19
20
21 **5-Methyl-N-(6-(thiomorpholinomethyl)quinolin-2-yl)-1-(*o*-tolyl)-1*H*-1,2,3-triazole-4-**
22 **carboxamide (3u).** The title compound was synthesized according to General Procedure
23
24 C (70%, a white solid): ¹H-NMR (400 MHz, CDCl₃) δ 9.90 (s, 1H), 8.53 (d, *J* = 8.4 Hz,
25
26 1H), 8.16 (d, *J* = 8.8 Hz, 1H), 7.85 (d, *J* = 8.4 Hz, 1H), 7.68-7.66 (m, 2H), 7.50-7.47 (m,
27
28 1H), 7.43-7.37 (m, 2H), 7.25 (d, *J* = 7.6 Hz, 1H), 3.66 (s, 2H), 2.74-2.69 (m, 8H), 2.50 (s,
29
30 3H), 2.06 (s, 3H); ¹³C-NMR (100 MHz, CDCl₃) δ 159.9, 150.4, 146.4, 138.8, 138.1, 137.8,
31
32 135.5, 135.1, 134.2, 131.5, 131.3, 130.9, 127.8, 127.1, 127.1, 126.1, 114.2, 63.4, 55.0, 28.0,
33
34 17.2, 9.3; HRMS (ESI): *m/z* [M + H]⁺ calcd for C₂₅H₂₇N₆OS, 459.1967; found, 459.1955.
35
36
37
38
39
40
41
42
43 HPLC: *t*_R = 2.12 min, 99.9%.

44
45
46 **2. Wnt-HEK293 Luciferase Reporter Assay in a 1536-Well Plate Format.** Stably
47
48 transfected Wnt-HEK293 cells were generated by transfection of HEK293 cells with TCF
49
50 based M50 Super 8x TOPFlash plasmid along with a pLenti-GFP-Puro empty plasmid
51
52 (Addgene). The clones carrying the TOPFlash and GFP constructs were screened with 2
53
54 μg/ml puromycin for a period of 3 weeks. Stably expressing clones were validated with
55
56
57

1
2
3 prototypical Wnt activators (WNT3a and LiCl) and inhibitor (XAV939). For our screening
4 studies, cells were dispensed at 2000/well in 4 μL of the Dulbecco's Modified Eagle
5 Medium supplemented with 10% fetal bovine serum into white-solid 1,536-well plates
6 (Greiner Bio-One North America Inc., Monroe, NC) using flying reagent dispenser (FRD,
7 Aurora Discovery, San Diego, CA). The assay plates were incubated for overnight at 37 $^{\circ}\text{C}$.
8 Then 23 nL of test compounds were transferred to the assay plates using pintool station
9 (Wako, San Diego, CA), followed by the addition of 1 μL of 200 ng/mL recombinant
10 human Wnt-3a (R&D Systems Inc., Minneapolis, MN) using an FRD to all the wells except
11 in the top half portions of the first four columns which received the control assay medium
12 instead. The assay plates were incubated for 24 h at 37 $^{\circ}\text{C}$. The cell viability was
13 determined as described below. For luciferase reporter assay, 4 μL /well ONE-Glo reagent
14 (Promega Corporation) was added using an FRD and luminescence signal was measured
15 through ViewLux plate reader after 30 min incubation at room temperature. Data were
16 expressed as relative fluorescence units (cell viability assay) and relative luminescence
17 units (luciferase reporter assay).
18
19
20
21
22
23
24
25
26
27
28
29
30
31
32
33
34
35
36
37

38 **3. Confirmatory Luciferase Reporter Assay in a 24-Well Plate Format.** Plasmids M50
39 Super 8x TOPFlash and FOPflash were gifts from Randall Moon (Addgene plasmid #
40 12456 and 12457).⁴⁸ Renilla luciferase was used as a control for the gene reporter assays.
41 Human pcDNA3-wild type and pcDNA3-S33Y β -catenin were gifts from Eric Fearon
42 (Addgene plasmid # 19286 and 16828).⁴⁹ HEK293 cells were transfected with the plasmids
43 for 16 h using lipofectamine 2000 (Qiagen). Compounds were incubated with the
44 transfected cells for additional 24 h and luciferase was measured using Promega's Dual-
45 Luciferase Reporter Assay System according to the manufacturer's directives. Calculations
46
47
48
49
50
51
52
53
54
55
56
57
58
59
60

1
2
3 were carried out by using the ratio of the TOPFlash or FOPFlash luciferase adjusted by the
4
5 Renilla luciferase.
6

7
8 **4. Determination of Cell Viability.** The effects of compounds on cell viability were
9
10 determined under two incubation conditions. First, the cell viability under the condition
11
12 for luciferase reporter assay was measured. The assay 1536-well plates were incubated
13
14 with a compound for 24 h at 37 °C. Then 1 µL/well CellTiter-Fluor reagent (Promega
15
16 Corporation, Madison, WI) was added using an FRD and fluorescence signal was measured
17
18 through ViewLux plate reader (Perkin Elmer, Boston, MA) after 30 min incubation at 37 °C.
19
20 Second, the cytotoxic effects of select compounds were assessed in unstimulated normal
21
22 HEK293 cells with inherently low background Wnt pathway activity. The cells were
23
24 plated at a density of 3.5×10^5 /well in 24-well plates for 24 h and then incubated with each
25
26 compound for a much longer incubation time of 72 h relative to that for the reporter assay.
27
28 Cell viability was determined by using CellTiter-Fluor reagent according to manufacturer's
29
30 instruction.
31
32
33
34
35

36 **5. Immunocytochemistry Analysis.** HEK293 cells were seeded on slides coated with
37
38 poly-D-lysine. In the following day, the cells were treated with compounds with or without
39
40 Wnt activation by 20 mM LiCl or Wnt3a conditioned medium. Then the cells were washed
41
42 once with PBS and fixed with 10% formalin (Sigma) at room temperature for 20 min. The
43
44 cells were permeabilized with methanol for 5 min and washed three times with PBS.
45
46 Blocking solution containing 5% bovine serum albumin in PBS was added to the slides for
47
48 1 h. Primary antibodies were incubated with the slide overnight and then secondary
49
50 antibodies were added for additional 2 h. Further wash step was carried out and DAPI was
51
52
53
54
55
56
57
58
59
60

1
2
3 incubated with the slide for 30 min. The slides were washed twice and mounted prior to
4
5 microscopy analysis.
6

7
8 **6. Cellular Fractionation and Western Blot Analysis.** Lysis of the cells were carried out
9
10 using lysis buffer (10 mM HEPES, 100 μ M EDTA, 10 mM KCl, 0.5% NP40, protease and
11
12 phosphatase inhibitor cocktails).⁵⁰ Cells were lysed for 20 min, vortexed for 10 seconds
13
14 and centrifuged at 13,000 x g for 15 min. Tissue lysis was carried out using RIPA Lysis
15
16 Buffer System (Santa Cruz Biotechnology, #sc-24948) and its fractionation was carried
17
18 out strictly as published by Wieckowski *et al.*⁵¹
19
20
21
22

23 Proteins were quantitated with bicinchoninic acid assay. The adjusted protein
24
25 concentrations were resolved on 10% SDS-PAGE gel. This was transferred to
26
27 nitrocellulose membrane and western blot was carried out using antibodies specific for the
28
29 proteins as followed: β -actin (Abcam) , p-catenin (#9561), Axin (#2087) were purchased
30
31 from Cell Signaling, and β -catenin (sc-133240), GSK-3 α/β (sc-7291) were from Santa
32
33 Cruz Biotechnology.
34
35
36

37 Overexpression pcDNA3 plasmid vectors for Flag tagged human beta-catenin and
38
39 beta-catenin S33Y were gifts from Eric Fearon (Addgene plasmid #19286).⁴⁹ All siRNAs
40
41 were purchased from Sigma-Adrich.
42
43
44

45 **7. Quantitative PCR.** Total RNA was extracted from cells or tissues using Trizol reagent
46
47 (Thermo Fisher) following the manufacturer's instructions. Reverse transcription was
48
49 carried out to obtain the complementary DNA, which was further used to determine the
50
51 gene expression using quantitative PCR. The human primers used in our studies are
52
53
54
55
56
57
58
59
60

1
2
3 outlined in Supplementary table 1 (Table S1) and those of the mouse have been previous
4
5 published.¹¹
6
7

8 **8. Immunoprecipitation.** Following experiments, cells were washed in PBS and scraped
9
10 into new Eppendorf tubes. Cell lysis was carried out with IP lysis buffer (25 mM Tris, 150
11
12 mM NaCl, 1 mM EDTA, 1% NP-40, 5% glycerol; pH 7.4) for 20 min. The lysates were
13
14 centrifuged at 13,000 x g for 15 min and the supernatant was collected and pellet discarded.
15
16 Protein A/G plus beads (Santa Cruz biotechnology) were added to preclear the lysate for 1
17
18 h. The lysate was centrifuge at 1,000 x g for 1 min and the supernatant was transferred to
19
20 a new Eppendorf tube. Protein concentration was determined with the BCA assay and 2
21
22 mg total protein was used for the immunoprecipitation experiment using the indicated
23
24 antibodies overnight. The protein beads were then added to the lysates and incubated for
25
26 12 h. The samples were centrifuge at 1,000 x g for 1 min and further washed with lysis
27
28 buffer three times. Laemmli sample buffer was added to the final pelleted beads. The
29
30 sample was heated at 95 °C for 5 min, then vortexed and centrifuge for additional 1 min.
31
32 The supernatant was immunoblotted for the indicated proteins.
33
34
35
36
37
38

39 **9. RNAi Mediated Knockdown.** All knockdown studies were carried out with
40
41 lipofectamine RNAimax (Thermofisher) for RNAi transfection according to
42
43 manufacturer's instructions. Small interfering RNAs were purchased from Sigma-Aldrich.
44
45 Cells were transfected for 36 h and treated with compounds for additional 24 h prior to
46
47 harvest unless otherwise indicated.
48
49
50

51 **10. Surface Plasmon Resonance (SPR) Analysis.** SPR assays were performed and
52
53 analyzed by the University of Maryland School of Medicine Biosensor Core Facility. GST
54
55 tagged human GSK3 β (#14-306-D) was purchased from Millipore Sigma.
56
57
58
59
60

1
2
3 **11. Nile Red Staining.** Huh7 cells were seeded on coverslips coated with rat Collagen I
4
5 overnight. The cells were then treated with varying concentrations of the compounds for
6
7 36 h and together with 200 μ M sodium oleate for additional 12 h. The Hanks' Balanced
8
9 Salt solution (HBSS) was used to wash the cells once and incubated with the cells along
10
11 with 1 μ M Nile red for 10 min at 37 °C in the dark. Excess Nile red was washed off with
12
13 HBSS buffer and the cells were imaged with a fluorescence microscope using 552/636 nm
14
15 (excitation/emission) lamp settings.
16
17
18

19
20 **12. Animals.** The animal experiments received prior approval from and followed the
21
22 guidelines of the Institutional Animal Care and Use Committee (IACUC) of the University
23
24 of Maryland Baltimore. All the mice were housed in 12-h light/ 12-h dark cycle with food
25
26 and water provided *ad libitum*. For the efficacy studies, mice were either fed a standard
27
28 normal chow diet or high fat diet (45% kcal fat) purchased from Harlan Laboratories
29
30 (Indianapolis, IN). All experiments utilized the *C57BL/6J* mice purchased from the
31
32 Jackson Laboratories (Bar Harbor, ME).
33
34
35

36
37 **13. Mouse Efficacy and Pharmacokinetic Study Design.** For the efficacy study, four
38
39 groups of 8 week-old male mice weighing 24-27 g were used for the experiments. Two
40
41 groups of mice were fed high fat diet obtained from Harlan Laboratories (#TD.08811)
42
43 containing 45% kcal fat initially for 6 weeks, then in combination with intraperitoneal
44
45 injection of 40 mg/kg compound **3a** or vehicle (corn oil) every two days until the end of
46
47 the experiments. The other two groups received normal chow diet throughout the study
48
49 with or without 40 mg/kg compound **3a**. Intraperitoneal glucose tolerance test (IPGTT)
50
51 was performed before and at the end of compound/vehicle treatment. Mice were sacrificed
52
53 one week after the second glucose tolerance test and about 24 h following the final dose.
54
55
56
57
58
59
60

1
2
3 For the pharmacokinetic evaluations, compound **3a** was dissolved at 1 mg/ml with 10%
4 Kolliphor EL and 10% Polyethylene Glycol in saline. Ten mice were separated into two
5
6 groups for intravenous and oral administration. Compound **3a** was given at 10 mg/kg to
7
8 the mice and blood samples were collected *via* tail vein at various time points and analyzed
9
10 by LC/MS/MS.
11
12
13

14
15 **14. Intraperitoneal Glucose Tolerance Test.** Mice were fasted for 6-8 h in new cages
16
17 without food. Following this, the mice were injected intraperitoneally glucose solution (2
18
19 g/kg) in saline. Glucometer was used to measure blood glucose levels from tail vein in a
20
21 time dependent manner.
22
23

24
25 **15. Triglyceride Assay.** Serum triglyceride level and liver triglyceride content were
26
27 quantitated using Triglyceride Quantitation Assay Kit (Abcam, #ab65336) following the
28
29 instructions from the manufacturer.
30
31

32
33 **16. Hematoxylin and Eosin Staining.** Tissue embedding and hematoxylin and eosin
34
35 staining was carried out by the University of Maryland School of Medicine Pathology Core
36
37 Facility.
38
39

40
41 **17. Serum Biochemical Analysis.** Comprehensive clinical biochemical assays to
42
43 determine metabolic status, liver and renal function were carried out by VRLTM-Maryland
44
45 (Gaithersburg, MD).
46
47
48
49
50
51
52
53
54
55
56
57
58
59
60

ASSOCIATED CONTENT

Supporting Information

The Supporting Information is available free of charge on the ACS Publication websites.

^1H and ^{13}C NMR spectra of new compounds and molecular formula strings and additional data.

AUTHOR INFORMATION

Corresponding Authors

*For Y.S.: phone, 410-706-7358; Email: yshu@rx.umaryland.edu

*For F.X.: phone, 410-706-8521; Email: fxue@rx.umaryland.edu

ACKNOWLEDGEMENTS

We thank the National Institute of General Medical Sciences of the US National Institutes of Health (NIH) for research support [R01GM099742] to Y.S. Dr. Yan Shu is a co-founder for and owns equity in Optivia Biotechnology. We also thank the Chinese National Natural Science Foundation [#21702073] to W.Y. and FX, and HuaiAn Science and Technology Bureau [HAC201706] to W.Y. and F.X. This work was supported in part by the Intramural Research Program of the National Center for Advancing Translational Sciences (NCATS).

ABBREVIATION USED

APC - Adenomatous polyposis coli

GSK3 β – Glycogen synthase kinase

LEF/TCF – T-cell factor/lymphoid enhancer factor

1
2
3 TCF7L2 – transcription factor 7 like 2
4

5 CK – Casein kinase
6

7 CBP - CREB-binding protein
8

9 FDA – food and drug administration
10

11 LiCl – lithium chloride
12

13 IPGTT – Intraperitoneal glucose tolerance test
14

15 HFD – high fat diet
16

17 NC – normal chow diet
18

19 AUC – Area under the curve
20

21 K_D – dissociation constant
22

23 IC_{50} - half-maximal inhibitory concentration
24
25
26
27
28
29
30
31
32
33
34
35
36
37
38
39
40
41
42
43
44
45
46
47
48
49
50
51
52
53
54
55
56
57
58
59
60

REFERENCES

- (1) Clevers, H.; Nusse, R. Wnt/ β -catenin signaling and disease. *Cell* **2012**, *149*, 1192-1205.
- (2) Valenta, T.; Hausmann, G.; Basler, K. The many faces and functions of β -catenin. *EMBO J.* **2012**, *31*, 2714-2736.
- (3) Oh, D. Y.; Olefsky, J. M. Medicine. Wnt fans the flames in obesity. *Science* **2010**, *329*, 397-398.
- (4) Bordonaro, M. Role of Wnt signaling in the development of type 2 diabetes. *Vitam. Horm.* **2009**, *80*, 563-581.
- (5) Schinner, S. Wnt-signalling and the metabolic syndrome. *Horm. Metab. Res.* **2009**, *41*, 159-163.
- (6) Grant, S. F.; Thorleifsson, G.; Reynisdottir, I.; Benediktsson, R.; Manolescu, A.; Sainz, J.; Helgason, A.; Stefansson, H.; Emilsson, V.; Helgadóttir, A.; Styrkarsdóttir, U.; Magnusson, K. P.; Walters, G. B.; Palsdóttir, E.; Jonsdóttir, T.; Gudmundsdóttir, T.; Gylfason, A.; Saemundsdóttir, J.; Wilensky, R. L.; Reilly, M. P.; Rader, D.J.; Bagger, Y.; Christiansen, C.; Gudnason, V.; Sigurdsson, G.; Thorsteinsdóttir, U.; Gulcher, J. R.; Kong, A.; Stefansson, K. Variant of transcription factor 7-like 2 (TCF7L2) gene confers risk of type 2 diabetes. *Nat. Genet.* **2006**, *38*, 320-323.
- (7) Gaulton, K. J.; Nammó, T.; Pasquali, L.; Simon, J. M.; Giresi, P. G.; Fogarty, M. P.; Panhuis, T. M.; Mieczkowski, P.; Secchi, A.; Bosco, D.; Berney, T.; Montanya, E.; Mohlke, K. L.; Lieb, J. D.; Ferrer, J. A map of open chromatin in human pancreatic islets. *Nat. Genet.* **2010**, *42*, 255-259.
- (8) Stitzel, M. L.; Sethupathy, P.; Pearson, D. S.; Chines, P. S.; Song, L.; Erdos, M. R.; Welch, R.; Parker, S. C.; Boyle, A. P.; Scott, L. J.; NISC Comparative Sequencing

1
2
3 Program, Margulies, E. H.; Boehnke, M.; Furey, T. S.; Crawford, G. E.; Collins, F. S.
4
5 Global epigenomic analysis of primary human pancreatic islets provides insights into type
6
7
8 2 diabetes susceptibility loci. *Cell Metab.* **2010**, *12*, 443-455.

9
10 (9) Lyssenko, V.; Lupi, R.; Marchetti, P.; Del Guerra, S.; Orho-Melander, M.; Almgren,
11
12 P.; Sjögren, M.; Ling, C.; Eriksson, K. F.; Lethagen, A. L.; Mancarella, R.; Berglund, G.;
13
14 Tuomi, T.; Nilsson, P.; Del Prato, S.; Groop, L. Mechanisms by which common variants
15
16
17 in the TCF7L2 gene increase risk of type 2 diabetes. *J. Clin. Invest.* **2007**, *117*, 2155-2163.

18
19 (10) Savic, D.; Ye, H.; Aneas, I.; Park, S. Y.; Bell, G. I.; Nobrega, M. A. Alterations in
20
21
22 TCF7L2 expression define its role as a key regulator of glucose metabolism. *Genome Res.*
23
24
25 **2011**, *21*, 1417-1425.

26
27 (11) Yang, H.; Li, Q.; Lee, J. H.; Shu, Y. Reduction in Tcf7l2 expression decreases diabetic
28
29
30 susceptibility in mice. *Int. J. Biol. Sci.* **2012**, *8*, 791-801.

31
32 (12) Ip, W.; Shao, W.; Chiang, Y. T.; Jin, T. The Wnt signaling pathway effector TCF7L2
33
34
35 is upregulated by insulin and represses hepatic gluconeogenesis. *Am. J. Physiol.*
36
37
38 *Endocrinol. Metab.* **2012**, *303*, E1166-1176.

39
40 (13) Shao, W.; Wang, D.; Chiang, Y. T.; Ip, W.; Zhu, L.; Xu, F.; Columbus, J.; Belsham,
41
42
43 D. D.; Irwin, D. M.; Zhang, H.; Wen, X.; Wang, Q.; Jin, T. The Wnt signaling pathway
44
45
46 effector TCF7L2 controls gut and brain proglucagon gene expression and glucose
47
48
49 homeostasis. *Diabetes* **2013**, *62*, 789-800.

50
51 (14) Boj, S. F.; van Es, J. H.; Huch, M.; Li, V. S.; José, A.; Hatzis, P.; Mokry, M.;
52
53
54 Haegerbarth, A.; van den Born, M.; Chambon, P.; Voshol, P.; Dor, Y.; Cuppen, E.; Fillat,
55
56
57 C.; Clevers, H. Diabetes risk gene and Wnt effector Tcf7l2/TCF4 controls hepatic response
58
59
60 to perinatal and adult metabolic demand. *Cell* **2012**, *151*, 1595-1607.

- 1
2
3 (15) Thompson, M. D.; Moghe, A.; Cornuet, P.; Marino, R.; Tian, J.; Wang, P.; Ma, X.;
4
5 Abrams, M.; Locker, J.; Monga, S. P.; Nejak-Bowen, K. β -Catenin regulation of farnesoid
6
7 X receptor signaling and bile acid metabolism during murine cholestasis. *Hepatology* **2018**,
8
9 *67*, 955-971.
10
11
12 (16) Popov, V. B.; Jornayvaz, F. R.; Akgul, E. O.; Kanda, S.; Jurczak, M. J.; Zhang, D.;
13
14 Abudukadier, A.; Majumdar, S. K.; Guigni, B.; Petersen, K. F.; Manchem, V. P.; Bhanot,
15
16 S.; Shulman, G. I.; Samuel, V. T. Second-generation antisense oligonucleotides against β -
17
18 catenin protect mice against diet-induced hepatic steatosis and hepatic and peripheral
19
20 insulin resistance. *FASEB J.* **2016**, *30*, 1207-1217.
21
22
23 (17) Kahn, M. Can we safely target the WNT pathway? *Nat. Rev. Drug Discov.* **2014**, *13*,
24
25 513-532.
26
27
28 (18) Polakis, P. Drugging Wnt signalling in cancer. *EMBO J.* **2012**, *31*, 2737-2746.
29
30
31 (19) Zimmerman, Z. F.; Moon, R. T.; Chien, A. J. Targeting Wnt pathways in disease. *Cold*
32
33 *Spring Harb. Perspect. Biol.* **2012**, *4*, a008086.
34
35
36 (20) Wodarz, A.; Nusse, R. Mechanisms of Wnt signaling in development. *Annu. Rev. Cell*
37
38 *Dev. Biol.* **1998**, *14*, 59-88.
39
40
41 (21) Ohishi, K.; Toume, K.; Arai, M. A.; Koyano, T.; Kowithayakorn, T.; Mizoguchi, T.;
42
43 Itoh, M.; Ishibashi, M. 9-Hydroxycanthin-6-one, a β -carboline alkaloid from eurycoma
44
45 longifolia, is the first Wnt signal inhibitor through activation of glycogen synthase kinase
46
47 3β without depending on casein kinase 1α . *J. Nat. Prod.* **2015**, *78*, 1139-1146.
48
49
50 (22) Lu, D.; Choi, M. Y.; Yu, J.; Castro, J. E.; Kipps, T. J.; Carson, D. A. Salinomycin
51
52 inhibits Wnt signaling and selectively induces apoptosis in chronic lymphocytic leukemia
53
54 cells. *Proc. Natl. Acad. Sci. U. S. A.* **2011**, *108*, 13253-13257.
55
56
57
58
59
60

1
2
3 (23) Hao, J.; Ao, A.; Zhou, L.; Murphy, C. K.; Frist, A. Y.; Keel, J. J.; Thorne, C. A.; Kim,
4 K.; Lee, E.; Hong, C. C. Selective small molecule targeting β -catenin function discovered
5 by in vivo chemical genetic screen. *Cell Rep.* **2013**, *4*, 898-904.
6
7

8
9
10 (24) Gwak, J.; Hwang, S. G.; Park, H. S.; Choi, S. R.; Park, S. H.; Kim, H.; Ha, N. C.; Bae,
11 S. J.; Han, J. K.; Kim, D. E.; Cho, J. W.; Oh, S. Small molecule-based disruption of the
12 Axin/ β -catenin protein complex regulates mesenchymal stem cell differentiation. *Cell Res.*
13 **2012**, *22*, 237-247.
14
15
16

17
18
19 (25) Huang, S. M.; Mishina, Y. M.; Liu, S.; Cheung, A.; Stegmeier, F.; Michaud, G. A.;
20 Charlat, O.; Wiellette, E.; Zhang, Y.; Wiessner, S.; Hild, M.; Shi, X.; Wilson, C. J.;
21 Mickanin, C.; Myer, V.; Fazal, A.; Tomlinson, R.; Serluca, F.; Shao, W.; Cheng, H.; Shultz,
22 M.; Rau, C.; Schirle, M.; Schlegl, J.; Ghidelli, S.; Fawell, S.; Lu, C.; Curtis, D.; Kirschner,
23 M. W.; Lengauer, C.; Finan, P. M.; Tallarico, J. A.; Bouwmeester, T.; Porter, J. A.; Bauer,
24 A.; Cong, F. Tankyrase inhibition stabilizes axin and antagonizes Wnt signalling. *Nature*
25 **2009**, *461*, 614-620.
26
27
28

29
30
31 (26) Henderson, W. R., Jr.; Chi, E. Y.; Ye, X.; Nguyen, C.; Tien, Y. T.; Zhou, B.; Borok,
32 Z.; Knight, D. A.; Kahn, M. Inhibition of Wnt/beta-catenin/CREB binding protein (CBP)
33 signaling reverses pulmonary fibrosis. *Proc. Natl. Acad. Sci. U. S. A.* **2010**, *107*, 14309-
34 14314.
35
36
37

38
39
40 (27) Toume, K.; Kamiya, K.; Arai, M. A.; Mori, N.; Sadhu, S. K.; Ahmed, F.; Ishibashi,
41 M. Xylogranin B: a potent Wnt signal inhibitory limonoid from *Xylocarpus granatum*. *Org.*
42 *Lett.* **2013**, *15*, 6106-6109.
43
44
45
46
47
48
49
50
51
52
53
54
55
56
57
58
59
60

1
2
3 (28) Lepourcelet, M.; Chen, Y. N.; France, D. S.; Wang, H. S.; Crews, P.; Petersen, F.;
4 Bruseo, C.; Wood, A. W.; Shivdasani, R. A. Small-molecule antagonists of the oncogenic
5 Tcf/beta-catenin protein complex. *Cancer Cell* **2004**, *5*, 91-102.

6
7
8
9
10 (29) Park, H. Y.; Toume, K.; Arai, M. A.; Sadhu, S. K.; Ahmed, F.; Ishibashi, M.
11 Calotropin: a cardenolide from *calotropis gigantea* that inhibits Wnt signaling by increasing
12 casein kinase 1 α in colon cancer cells. *Chembiochem* **2014**, *15*, 872-878.

13
14
15 (30) García-Reyes, B.; Witt, L.; Jansen, B.; Karasu, E.; Gehring, T.; Leban, J.; Henne-Bruns, D.;
16 Pichlo, C.; Brunstein, E.; Baumann, U.; Wesseler, F.; Rathmer, B.; Schade, D.; Peifer, C.;
17 Knippschild, U. Discovery of inhibitor of Wnt Production 2 (IWP-2) and related compounds as
18 selective ATP-competitive inhibitors of Casein Kinase 1 (CK1) δ/ϵ . *J. Med. Chem.* **2018**, *61*, 4087-
19 4102.

20
21
22 (31) Cha, P. H.; Cho, Y. H.; Lee, S. K.; Lee, J.; Jeong, W. J.; Moon, B. S.; Yun, J. H.;
23 Yang, J. S.; Choi, S.; Yoon, J.; Kim, H. Y.; Kim, M. Y.; Kaduwal, S.; Lee, W.; Min do, S.;
24 Kim, H.; Han, G.; Choi, K. Y. Small-molecule binding of the axin RGS domain promotes β -
25 catenin and Ras degradation. *Nat. Chem. Biol.* **2016**, *12*, 593-600.

26
27
28 (32) Liu, J.; Pan, S.; Hsieh, M. H.; Ng, N.; Sun, F.; Wang, T.; Kasibhatla, S.; Schuller, A.
29 G.; Li, A. G.; Cheng, D.; Li, J.; Tompkins, C.; Pferdekamper, A.; Steffy, A.; Cheng, J.;
30 Kowal, C.; Phung, V.; Guo, G.; Wang, Y.; Graham, M. P.; Flynn, S.; Brenner, J. C.; Li,
31 C.; Villarroel, M. C.; Schultz, P. G.; Wu, X.; McNamara, P.; Sellers, W. R.; Petruzzelli,
32 L.; Boral, A. L.; Seidel, H. M.; McLaughlin, M. E.; Che, J.; Carey, T. E.; Vanasse, G.;
33 Harris, J. L. Targeting Wnt-driven cancer through the inhibition of Porcupine by LGK974.
34
35
36
37
38
39
40
41
42
43
44
45
46
47
48
49
50
51
52
53
54
55
56
57
58
59
60
Proc. Natl. Acad. Sci. U. S. A. **2013**, *110*, 20224-20229.

(33) Madan, B.; Ke, Z.; Harmston, N.; Ho, S. Y.; Frois, A. O.; Alam, J.; Jeyaraj, D. A.;
Pendharkar, V.; Ghosh, K.; Virshup, I. H.; Manoharan, V.; Ong, E. H.; Sangthongpitag,

1
2
3 K.; Hill, J.; Petretto, E.; Keller, T. H.; Lee, M. A.; Matter, A.; Virshup, D. M.; Wnt
4 addiction of genetically defined cancers reversed by PORCN inhibition. *Oncogene* **2016**,
5
6 *35*, 2197-2207.
7
8

9
10 (34) Mo, M. L.; Li, M. R.; Chen, Z.; Liu, X. W.; Sheng, Q.; Zhou, H. M. Inhibition of the
11
12 Wnt palmitoyltransferase porcupine suppresses cell growth and downregulates the Wnt/ β -
13
14 catenin pathway in gastric cancer. *Oncol. Lett.* **2013**, *5*, 1719-1723.
15
16

17 (35) Lu, W.; Lin, C.; Roberts, M. J.; Waud, W. R.; Piazza, G. A.; Li, Y. Niclosamide
18
19 suppresses cancer cell growth by inducing Wnt co-receptor LRP6 degradation and
20
21 inhibiting the Wnt/ β -catenin pathway. *PLoS One* **2011**, *6*, e29290.
22
23

24 (36) Thorne, C. A.; Hanson, A. J.; Schneider, J.; Tahinci, E.; Orton, D.; Cselenyi, C. S.;
25
26 Jernigan, K. K.; Meyers, K. C.; Hang, B. I.; Waterson, A. G.; Kim, K.; Melancon, B.;
27
28 Ghidu, V. P.; Sulikowski, G. A.; LaFleur, B.; Salic, A.; Lee, L. A.; Miller, D. M. 3rd; Lee,
29
30 E. Small-molecule inhibition of Wnt signaling through activation of casein kinase 1 α . *Nat.*
31
32 *Chem. Biol.* **2010**, *6*, 829-836.
33
34

35 (37) Shinoda, K.; Ohyama, K.; Hasegawa, Y.; Chang, H. Y.; Ogura, M.; Sato, A.; Hong,
36
37 H.; Hosono, T.; Sharp, L. Z.; Scheel, D. W.; Graham, M.; Ishihama, Y.; Kajimura, S.
38
39 Phosphoproteomics identifies CK2 as a negative regulator of beige adipocyte
40
41 thermogenesis and energy expenditure. *Cell Metab.* **2015**, *22*, 997-1008.
42
43

44 (38) Rossi, M.; Ruiz de Azua, I.; Barella, L. F.; Sakamoto, W.; Zhu, L.; Cui, Y.; Lu, H.;
45
46 Rebholz, H.; Matschinsky, F. M.; Doliba, N. M.; Butcher, A. J.; Tobin, A. B.; Wess, J.
47
48 CK2 acts as a potent negative regulator of receptor-mediated insulin release in vitro and in
49
50 vivo. *Proc. Natl. Acad. Sci. U. S. A.* **2015**, *112*, E6818-6824.
51
52
53
54
55
56
57
58
59
60

1
2
3 (39) Zhong, L.; Ding, Y.; Bandyopadhyay, G.; Waaler, J.; Börgeson, E.; Smith, S.; Zhang,
4 M.; Phillips, S. A.; Mahooti, S.; Mahata, S. K.; Shao, J.; Krauss, S.; Chi, N. W. The
5 PARsylation activity of tankyrase in adipose tissue modulates systemic glucose
6 metabolism in mice. *Diabetologia* **2016**, *59*, 582-591.
7

8
9
10
11 (40) Smith, T. C.; Kinkel, A. W.; Gryczko, C. M.; Goulet, J. R. Absorption of pyrvinium
12 pamoate. *Clin. Pharmacol. Ther.* **1976**, *19*, 802-806.
13
14

15
16 (41) Zhu, W.; Groh, M.; Hauptenthal, J.; Hartmann, R. W. A detective story in drug
17 discovery: elucidation of a screening artifact reveals polymeric carboxylic acids as potent
18 inhibitors of RNA polymerase. *Chemistry* **2013**, *19*, 8397-8400.
19
20
21

22
23 (42) Baell, J. B.; Holloway, G. A. New substructure filters for removal of pan assay
24 interference compounds (PAINS) from screening libraries and for their exclusion in
25 bioassays. *J. Med. Chem.* **2010**, *53*, 2719-2740.
26
27
28

29
30 (43) Martino-Echarri, E.; Brocardo, M. G.; Mills, K. M.; Henderson, B. R. Tankyrase
31 inhibitors stimulate the ability of tankyrases to bind axin and drive assembly of β -catenin
32 degradation-competent axin puncta. *PLoS One* **2016**, *11*, e0150484.
33
34
35

36
37 (44) Rowan, A. J.; Lamlum, H.; Ilyas, M.; Wheeler, J.; Straub, J.; Papadopoulou, A.;
38 Bicknell, D.; Bodmer, W. F.; Tomlinson, I. P. APC mutations in sporadic colorectal
39 tumors: A mutational "hotspot" and interdependence of the "two hits". *Proc. Natl. Acad.*
40 *Sci. U. S. A.* **2000**, *97*, 3352-3357.
41
42
43
44

45
46 (45) de La Coste, A.; Romagnolo, B.; Billuart, P.; Renard, C. A.; Buendia, M. A.;
47 Soubrane, O.; Fabre, M.; Chelly, J.; Beldjord, C.; Kahn, A.; Perret, C. Somatic mutations
48 of the beta-catenin gene are frequent in mouse and human hepatocellular carcinomas. *Proc.*
49 *Natl. Acad. Sci. U. S. A.* **1998**, *95*, 8847-8851.
50
51
52
53

1
2
3 (46) Zhang, Y. L.; Guo, H.; Zhang, C. S.; Lin, S. Y.; Yin, Z.; Peng, Y.; Luo, H.; Shi, Y.;
4 Lian, G.; Zhang, C.; Li, M.; Ye, Z.; Ye, J.; Han, J.; Li, P.; Wu, J. W.; Lin, S. C. AMP as a
5 low-energy charge signal autonomously initiates assembly of AXIN-AMPK-LKB1
6 complex for AMPK activation. *Cell Metab.* **2013**, *18*, 546-555.
7
8
9

10
11 (47) Behari, J.; Li, H.; Liu, S.; Stefanovic-Racic, M.; Alonso, L.; O'Donnell, C. P.; Shiva,
12 S.; Singamsetty, S.; Watanabe, Y.; Singh, V. P.; Liu, Q. β -catenin links hepatic metabolic
13 zonation with lipid metabolism and diet-induced obesity in mice. *Am. J. Pathol.* **2014**, *184*,
14 3284-3298.
15
16
17
18
19

20
21 (48) Veeman, M. T.; Slusarski, D. C.; Kaykas, A.; Louie, S. H.; Moon, R. T. Zebrafish
22 prickle, a modulator of noncanonical Wnt/Fz signaling, regulates gastrulation movements.
23 *Curr. Biol.* **2003**, *13*, 680-685.
24
25
26
27

28 (49) Kolligs, F. T.; Hu, G.; Dang, C. V.; Fearon, E. R. Neoplastic transformation of RK3E
29 by mutant beta-catenin requires deregulation of Tcf/Lef transcription but not activation of
30 c-myc expression. *Mol. Cell. Biol.* **1999**, *19*, 5696-5706.
31
32
33
34

35 (50) Schreiber, E.; Harshman, K.; Kemler, I.; Malipiero, U.; Schaffner, W.; Fontana, A.
36 Astrocytes and glioblastoma cells express novel octamer-DNA binding proteins distinct
37 from the ubiquitous Oct-1 and B cell type Oct-2 proteins. *Nucleic Acids Res.* **1990**, *18*,
38 5495-5503.
39
40
41
42
43

44 (51) Wieckowski, M. R.; Giorgi, C.; Lebedzinska, M.; Duszynski, J.; Pinton, P. Isolation
45 of mitochondria-associated membranes and mitochondria from animal tissues and cells.
46 *Nat. Protoc.* **2009**, *4*, 1582-1590.
47
48
49
50
51

TABLE OF CONTENTS GRAPHIC

